Mechanisms of Improving Collateral Blood Flow During Ischemic Stroke

Undergraduate Honors Research Thesis

Presented in Partial Fulfillment of the Requirements for graduation
"with Honors Research Distinction" in the undergraduate School of Arts and Science of
The Ohio State University

By:
Seth Teplitsky

The Ohio State University

April 2014

Project Advisor: Professor Dr. Cameron Rink, Department of Surgery

Thesis Committee:
Dr. Cameron Rink, Ph.D, Advisor
Dr. Savita Khanna, Ph.D
Dr. Ciaran Powers, Ph.D, MD

Abstract:

More than 795,000 Americans suffer a stroke annually, and it is the third leading cause of death in the United States[1]. There are two types of stroke, hemorrhagic and ischemic. Hemorrhagic stroke is caused by the rupture of blood vessels within the brain, as opposed to ischemic strokes, which are caused by a blockage within the vessel. Of all strokes presented clinically, 86% are ischemic by nature[1]. Currently, there are few treatments for ischemic stroke. The prevailing early treatments include thrombolytic therapy and antiplatelet therapy such as low dose aspirin[2,3]. These treatments are each flawed. Tissue plasminogen activator (tPA) is currently the only FDA-approved thrombolytic therapy for the acute treatment of ischemic stroke[4]. This treatment is approved for less than 10% of patients, and is given to less than 4%[4]. In addition, greater than 65% of hospitals in America have never administered tPA to patients due to low efficacy as well as potential harmful side effects[5]. Antiplatelets, such as low dose aspirin, are another treatment option. These are drugs, and therefore have negative side effects associated with long-term use such as increased risk of hemorrhagic stroke[6], and gastrointestinal bleeding[7]. As a result, there is a distinct lack of safe therapeutic options for both the early and long-term treatment of ischemic stroke patients.

Cerebrovascular collaterals refer to the network of blood vessels that are clinically documented to perfuse stroke-affected tissue during ischemic stroke and reduce brain injury[8]. While strategies to improve collateral blood flow during stroke are of significant therapeutic interest, mechanisms and a means to improve circulation

through these blood vessels during stroke remain unknown. This honors thesis proposal rests on a key *in vivo* observation that supplementation of a lesser-characterized natural vitamin E, alpha-tocotrienol (TCT), improves cerebrovascular collateral blood flow and attenuates stroke injury[8]. TCT therefore serves as a powerful tool to study cerebrovascular collateral remodeling during stroke. The overall objective of this honors thesis will be to characterize the effects of TCT on cerebrovascular collateral perfusion during stroke and to identify a mechanistic basis for TCT improvement of cerebrovascular collateral circulation. Many previously identified arteriogenic markers, including Tissue inhibitor of metalloproteinase 1 (TIMP1), will be investigated as a known molecular target of interest for induction of collateral growth in the brain. FITC-lectin tagging of cerebrovascular collaterals will be used for laser capture microdissection experiments and downstream molecular study of arteriogenic targets. This approach will enable the specific collection of perfused cerebrovascular collaterals from stroke-affected tissue for mechanistic study.

Acknowledgements

I would like to sincerely thank my advisor Dr. Cameron Rink. He has been an exceptional mentor, thoroughly peaking my interest in research, and aided me through every step of the process leading to the completion of this project, for which I am extremely grateful. Additionally, I would like to thank all the lab members who have helped train me along the way, and provided the necessary resources along the way. Specifically, I would like to recognize Kevin Olickal and Mallory Hiegel, for their important contributions to this project. Lastly, I would like to express my gratitude to the other committee members, Dr. Savita Khanna and Dr. Ciaran Powers. The time and energy put in to helping me complete this thesis was greatly appreciated and not unnoticed.

Table of Contents

List of Tables:

List of Figures:

19. **MMP2 mRNA expression from laser captured collaterals**
20. **MMP9 mRNA expression from laser captured collaterals**
21. **TIMP1 mRNA expression from laser captured collaterals**
22. **TIMP2 mRNA expression from laser captured collaterals**
23. **CLIC1 mRNA expression from laser captured collaterals**
24. **CLIC4 mRNA expression from laser captured collaterals**
25. **KLF2 mRNA expression from laser captured collaterals**
26. **RT-PCR amplification plot of CD44v3**
27. **PCAF mRNA expression from laser captured collaterals**
28. **EphrinB2 mRNA expression from laser captured collaterals**
29. **Delta-Like 1 mRNA expression from laser captured collaterals**
30. **Delta-Like 4 mRNA expression from laser captured collaterals**
31. **Schematic representation of arteriogenesis and the studied markers**

Introduction:

Vitamin E: Discovery and Characterization. Vitamin E was discovered in 1922 by Herbert Evans[9] when he identified phytochemical factors essential for rodent reproduction. This work was later continued by Barnett Sure who extrapolated its importance to humans, and named it "vitamin E" according to the micronutrient naming conventions of the time[10]. The chemical name assigned for the molecule was tocopherol, stemming from the Greek term for childbirth, which is "tocos"[11]. Vitamin E's importance was not fully understood until more modern technology and theory of the 1950's allowed for its elucidation in the context of the developing field of redox biology.

Palm oil provides the greatest source of a lesser-characterized vitamin E isomer, α-tocotrienol, which has antioxidant effects as well as antioxidant-independent health benefits shown to affect a broad range of pathological disorders[11]. Crude palm oil contains up to 800 mg/kg by weight of the α-tocotrienol isomer[12]. Palm oil has been documented in human diet as far back as 3000 BC[9], but did not become prevalent in diet until the early 20th century. The palm oil comes from the fruits of the oil palm tree, *Elaeis* guineensis[12]. The oil accounts for about 30% of the world's total oil production[13], with the most recent annual output of 58.2 million tons[14]. This oil is primarily produced in Southeast Asia[15], specifically Malaysia and Indonesia, and is still relatively scarce in western diet despite its growing prominence and production on a global scale. This is likely due to the oils higher content of saturated fatty acids (SFA) when compared to other common vegetable oils[16], which is assumed to cause an increase in low density

lipoprotein (LDL) cholesterol as increased SFA are known to do[17]. There is however conflicting scientific evidence of this outcome from oil-rich diets[18,19].

Today vitamin E is known to consist of eight isomers divided into two families, tocopherols as discovered by Evans, and tocotrienols as discovered by Pennock and Whittle in 1963[20]. Tocopherols consist of a chromanol ring and a 15-carbon saturated tail derived from homogentisate (HGA) and phytyl diphosphate, respectively[21]. The tocotrienols possess the same chromanol head structure, varying only in the carbon tail where they contain 3 trans doubles bonds at positions 3', 7', and 11'. Both compound families contain α, β, ɣ, and δ isoforms, differing in position and degree of methylation on the chromanol head of the compound (**Figure 1**). In addition to structural differences, a growing body of scientific literature[11,21] supports independent biological functions for vitamin E family members, some of which are known to be independent of its classically defined antioxidant function.

Key differences between tocopherol and tocotrienol family members. When the two families are compared, their prevalence in the plant kingdom is unequal. Tocopherols as compared to tocotrienols are much more abundant in nature[22-24]. The tocopherols are mainly found in the leaves and seeds of most dicots, and are present as the prominent vitamin E component, whereas the tocotrienols are mainly found in the seeds of most monocots and a limited number of dicots[25]. More detailed analysis has been done to show that tocotrienols are mainly focused in non-photosynthetic tissue[25]. In light of the unique biological distribution of vitamin E family members, growing

evidence supports unique biological function for tocopherols and tocotrienols as well. The research that has focused on the lesser-characterized forms of Vitamin E lends support to unique biological function compared to α-tocopherol. Such biological functions seen in tocotrienols but not tocopherols include inhibition of HMG-CoA Reductase, the same enzyme targeted by the statin class of drugs that is responsible for cholesterol synthesis[26,27]. Tocotrienol vitamin E has also been reported to inhibit growth of human breast cancer[28], and protect neurons from ischemic stroke induced brain injury[29]. The study of these lesser-characterized forms of vitamin E remained relatively untouched until the past decade. While the most bioavailable form of vitamin E, α-tocopherol, is well studied and has a known selective transport system in mammals, little remains known about tocotrienol uptake and transport. It is estimated that only 1% of all the vitamin E research produced in the last 30 years pertains to tocotrienols[11]. The current work aims to further the findings of unique, anti-oxidant independent functions within the lesser-studied vitamin E isomers.

Research efforts related to ischemic stroke and the process of arteriogenesis have increased dramatically over the past twenty-five years. A search of available literature using “ischemic stroke” as a key term in PubMed revealed 23,302 publications in the quarter century period of 1980–2004. By comparison, in the past decade alone there have been 34,268 articles published (2005 through February 2014, **Figure 2**). During the same time periods, a PubMed search using arteriogenesis as the key word revealed only 202 publications in the twenty-five year period spanning 1980–2004. In the past decade, however, there have been 544 published (**Figure 3)**. A similar trend was

observed using tocotrienol as a keyword (**Figure 4**). Taken together, the dramatic increase in publication efforts across these distinct disciplines suggests growing clinical and patient awareness. As it specifically relates to arteriogenesis, primary literature addressing current molecular targets for arteriogenesis has been reviewed for the purpose of screening TCT sensitive arteriogenic factors (**Table 1**). The summarizing table is organized by target, and briefly describes their known role in arteriogenic remodeling of collaterals.

Tocotrienol and Neuroprotection. The biological significance of vitamin E was developed on the basis of its antioxidant function as the body's primary lipid soluble defense mechanism against oxidative stress and injury[30]. As the vitamin E family grew with the identification of new naturally occurring isoforms (i.e. tocotrienols), so did research efforts elucidating antioxidant independent biological function. For example, a recent and growing body of research on the lesser-characterized isomer, alpha-tocotrienol, has identified neuroprotective properties against both glutamate and stroke induced neurodegeneration at nanomolar quantities. Importantly, these properties are unique to alpha-tocotrienol, as the better-characterized alpha-tocopherol does not possess these effects in the nanomolar concentration range[29]. Any biological activity at this concentration cannot be attributed to antioxidant function, as other lipid soluble antioxidants are present in brain tissue at much higher quantity[11]. This observation points to specific mechanisms of biological function for vitamin E family members that are unrelated to their well-known role as antioxidants.

Multimodal Tocotrienol Protection Against Ischemic Stroke. In light of the failure of neuroprotective agents in rodent stroke models to translate to clinical success, the TCT-dependent protection observed in rodent models had to be tested in a large animal setting before going to patient trials. Outcomes of a large animal (canine) trial validated prophylactic supplementation of TCT for protection of grey and white matter brain tissue against acute ischemic stroke[31]. The study demonstrated a significant decrease in post-stroke infarct size from those animals supplemented with TCT as opposed to the placebo control[31]. Furthermore, an unexpected finding was uncovered in the canine study that was enabled by real-time angiography of cerebral blood flow. Prior to this work, cerebral angiography was not investigated in rodent stroke models testing TCT. Strikingly, retrospective review of cerebral angiograms identified improved collateral blood flow in stroke-affected tissue of TCT supplemented canines as compared to placebo controls. Quantitative analyses of collateral blood flow was determined from cerebral angiograms using an 11-point clinical scale. Of interest, stroke-induced lesion volume correlated tightly with collateral score, such that the canines supplemented with TCT had greater collateral blood flow and smaller stroke lesion volumes[31].

From here, the current work moves back to small animal models in order to find the mechanistic basis for how TCT improves cerebrovascular collateral blood flow and attenuates stroke injury. It is hypothesized that the collateral blood flow improvement found from supplementation of α-tocotrienol is a results of arteriogenesis. Arteriogenesis refers to the remodeling of pre-existing collateral blood vessels, whereas angiogenesis is the growth of new collateral blood vessels altogether. To study the mechanistic basis

of improved collateral blood flow via arteriogenesis, previously identified arteriogenic factors including tissue inhibitor of metalloproteinase 1 (TIMP1), and matrix metalloproteinase 9 (MMP9) were studied as known molecular targets of interest[32,33]. TIMP1 plays the role of inhibitor to the MMP family. The MMP family of peptidases is known to break down the proteins that keep the endothelial cells intact, therefore the hypothesis is that inhibition of the family results in arteriogenesis and increased blood flow. Increased MMP activity is assumed to lead to tipping the balance towards a pro-proteolytic environment causing a decrease in mature collaterals, while increased TIMP expression will cause decreased MMP activity, and henceforth lead to an anti-proteolytic environment where there is an increase in mature collaterals. Indeed, it has already been published that cerebral arteriogenesis induced by stroke causes an up-regulation of TIMP1 in collaterals[31,33]. Outcomes from our canine work support this claim following 10 weeks of prophylactic TCT supplementation. The current work seeks to determine earlier changes in pro-arteriogenic target gene expression, including TIMP1 and the aforementioned targets listed in Table 1. Briefly, mice were supplemented prophylactically with TCT or vehicle placebo for 4-6 weeks prior to mechanical occlusion of the middle cerebral artery to cause ischemic stroke in primary somatosensory cortex. We describe a new technique to label collaterals during ischemia and leverage experience with laser capture microdissection to selectively measure gene expression of arteriogenic targets in collected perfused collaterals.

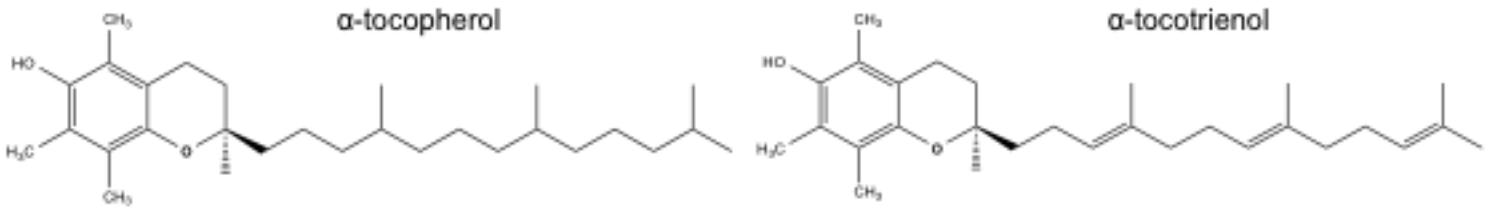

Figure. 1. Chemical structure of α-tocopherol and α-tocotrienol. The three unsaturation points at carbon positions 3, 7, and 11 can be seen on the side chain.

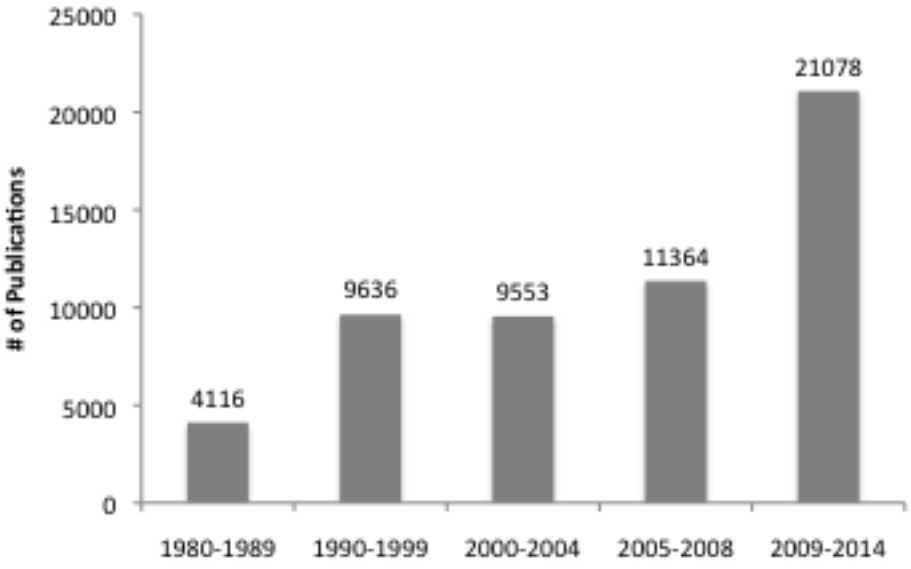

Figure 2. Ischemic stroke publications over time. Number of publications related to ischemic stroke from 1980 to 2014. Search words: Ischemic Stroke. Search performed on March 3 2014, including ahead of print publications. Databases: Pubmed.

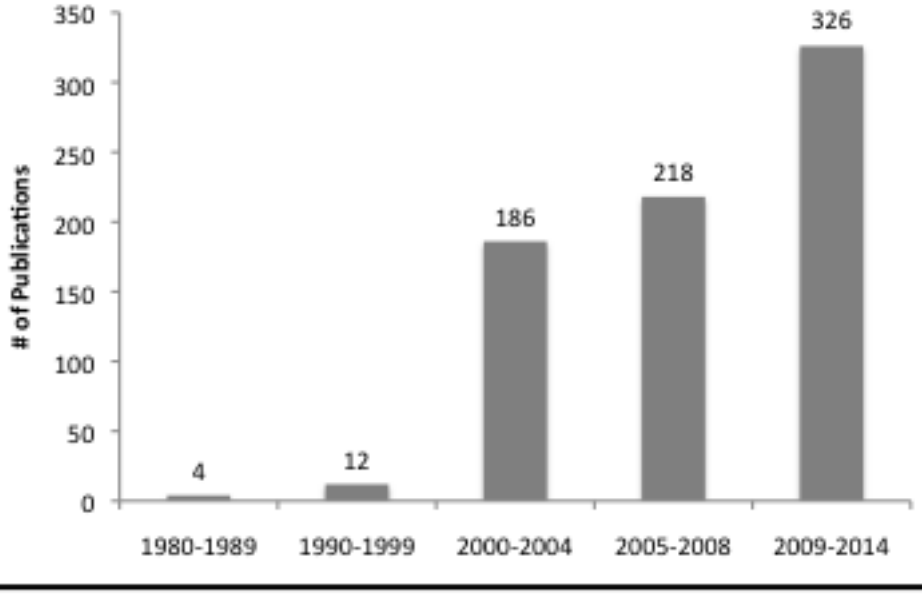

Figure 3. Arteriogenesis publications over time. Number of publications related to arteriogenesis from 1980 to 2014. Search words: Arteriogenesis. Search performed on March 3 2014, including ahead of print publications. Databases: Pubmed.

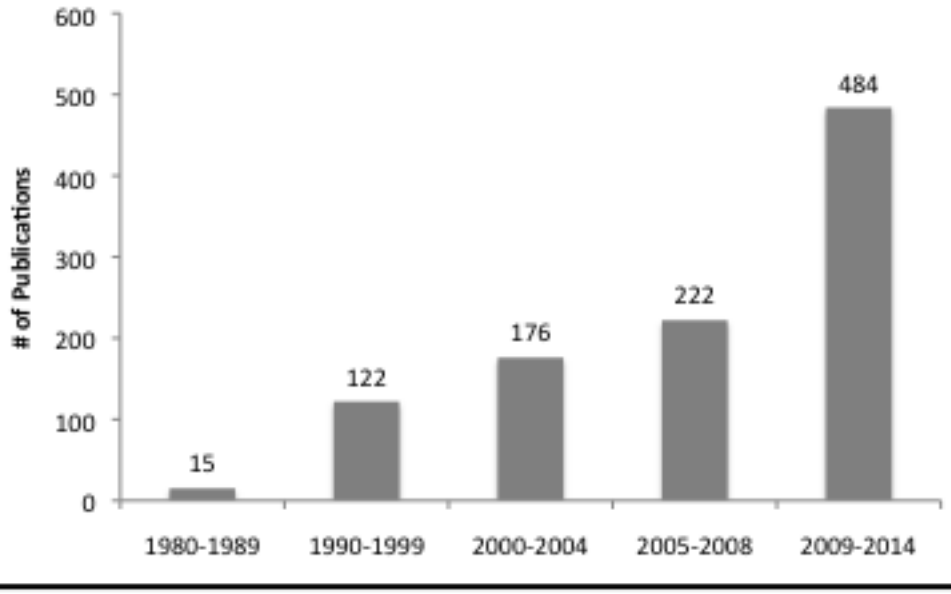

Figure 4. Tocotrienol publications over time. Number of publications related to tocotrienol from 1980 to 2014. Search words: Tocotrienol. Search performed on March 4 2014, including ahead of print publications. Databases: Pubmed.

Gene Markers	Full Name	Role in Arteriogenesis	Reference
MMP2, MMP9	Matrix Metalloproteinase	Breakdown of extracelular matrix	(Cai and Schafer, 2008)
TIMP1, TIMP2	Tissue Inhibitor of Metalloproteinase	Inhibition of MMP, maintenance of proteolytic environment	(Nagase et al. 2006)
CLIC1, CLIC4	Chloride Intracellular Channel	Endothelial cell hollowing allowing for vessel widening (also referred to as tubulogenesis)	(Chalothorn et al. 2009)
KLF2	Krüppel-like Factor 2	Responsive to fluid shear forces allowing it to act as a hemodynamic regulator	(Lee et al. 2006)
CD44v3	Cluster of Differentiation 44 variant 3	Facilitates preservation of growth factors	(Bot et al. 2013)
KAT2B	K(Lysine) Acetyltransferase 2B	PCAF acts as master switch in the inflammatory processes required for effective arteriogenesis	(Bastiaansen et al. 2013)
Shc1	Src homology 2 domain containing Transforming Protein 1	Activation of Notch and NF-κB signaling pathway, both critical for inflammation and arterial specification	(Sweet et al. 2013)
DLL1	Delta-like Ligand 1		
DLL3	Delta-like Ligand 4		
EFNB2	Ephrin-B2		
PECAM1	Platelet Endothelial Cell Adhesion Molecule 1	Acts as an important regulator of shear stress–induced cell alignment	(Chen et al. 2010)

Table 1. Primary literature reviews on arteriogenic factors

Methods:

Animal Supplementation. All experiments were approved by the Institutional Animal Care and Use Committee of the Ohio State University. Upon arrival, twelve C57BL/6 (5-week old, Harlan, Indianapolis, USA) mice were allowed to acclimate to their home cage environment for 1 week prior to supplementation. At the start of supplementation, mice were randomized to one of two groups (n=6). Group one received supplementation for 4 weeks and group two received supplementation for 6 weeks. Mice were maintained under standard vivarium conditions (22±2°C with 12:12 dark: light hour cycles). Within groups, mice were evenly divided to receive placebo control (n=3) or TCT (n=3) supplementation. The placebo group was orally gavaged five days a week with vitamin E stripped corn oil using a volume matched to the mean of TCT supplemented mice (**Figure 5**). The test group was orally gavaged with TCT (Carotech, Malaysia) in vitamin E-stripped corn oil at a dosage of 50 mg/kg body weight as reported previously[29]. Surgery was performed at 24h after the last supplementation.

Surgery. Acute ischemic stroke was induced using the intraluminal suture method of middle cerebral artery occlusion (MCAO) as described previously[29] (**Figure 6**). Transient focal cerebral ischemia was induced in mice following 4 or 6 weeks of supplementation. The mice were anesthetized with 1 to 1.5% isoflurane delivered by medical air (21% O_2, balance N_2). A monofilament nylon suture (6-0) was advanced into the internal carotid artery by way of the external carotid artery. The filament tip was directed until slight resistance was felt (~8 mm). Cortical blood flow was continuously

monitored during surgery using laser Doppler flowmetry (LDF). Successful MCAO was confirmed by a >70% reduction in relative blood flow in the MCA supplied cortex. Once MCAO was validated, the mice remained under anesthesia for 30min until FITC-lectin perfusion was performed while MCAO-induced ischemia persisted.

Validation of acute ischemic stroke surgical model. Acute ischemic stroke is caused by an abrupt and sudden occlusion of a large vessel which arrests cerebral blood flow and the delivery of blood borne nutrients including oxygen and glucose to brain tissue. To model this phenomenon *in vivo*, we employed the intraluminal suture method of middle cerebral artery occlusion (MCAO, as depicted in **Figure 6** of methods). This approach induces ischemic stroke by mechanical occlusion of the MCA using a 6-0 nylon filament suture[29]. As real-time cerebral angiography is not enabled in our rodent model, we rely on laser Doppler flowmetry (LDF) to validate successful MCA occlusion. To acquire LDF from the occluded MCA territory, a 5mm incision is made in the scalp for intracranial LDF probe placement. The probe is placed in the primary somatosensory (S1) cortex using a small screw affixed with cyanoacrylate. LDF produces continuous light (785nm), and gives measurements in arbitrary perfusion units (pfu). In order to determine the decrease in blood flow using LDF, before the suture is inserted into the middle cerebral artery, cortical blood flow is monitored to establish a pre-stroke baseline. Once MCAO is successfully performed, blood flow is continuously monitored, and successful occlusion is confirmed by a >70% reduction in relative blood flow as compared to baseline. The table shown gives an exact percentage decrease in cortical blood flow seen by each animal during surgery, conferring successful stroke in each.

FITC-Perfusion. FITC-conjugated lectin (tomato *Lycopersicon esculentum*, Vector Laboratories) was perfused during ischemia to visualize perfused collaterals of the stroke-affected S1 cortex for use with laser capture microdissection experiments and downstream molecular study. Mice remained anesthetized with isoflurane (1%–1.5%) in medical air and FITC-lectin perfusion was performed while the MCA remained occluded. Delivery of FITC-lectin particles during cerebral ischemia was achieved by intracardial injection (250μL FITC-lectin) 30mins after the onset of MCAO. FITC-lectin was allowed to circulate systemically for 5min after which deeply anesthetized mice were decapitated and brain tissue collected and embedded in OCT (Sakura, Torrance, CA, USA). Cerebellum brain tissue was snap frozen in liquid nitrogen for downstream HPLC determination of vitamin E content.

Vitamin E Extraction and Analysis Using High Performance Liquid Chromatography. Vitamin E extraction (**Table 2**) and analysis of mouse brain tissue was performed as previously described using an HPLC-coulometric electrode array detector (Coularray Detector, 12-channel, model 5600, ESA, Chelmsford, MA, USA) (**Figure 7**). This system enables the simultaneous detection of five naturally occurring vitamin E family members in a single run[34] (**Figure 8**), including alpha-tocopherol, gamma-tocopherol, alpha-tocotrienol, gamma-tocotrienol, and delta-tocotrienol.

Immunohistochemistry and imaging. At the time of euthanasia, mouse cerebral hemispheres were sliced in the coronal axis using a brain matrix (Ted Pella, Inc.) and

embedded in OCT (**Figure 9**). OCT-embedded frozen brain tissue was sectioned (10μm) using a cryostat (CM3050s, Leica Microsystems, Buffalo Grove, IL, USA) and mounted on positive-charged slides. Immunohistochemical staining of sections was performed as described[35] using CD31 (1:200; BD Pharmingen, San Diego, CA, USA) primary antibody to label all blood vessels in the stroke-affected hemisphere regardless of whether they were perfused. Secondary antibody detection and counterstaining were performed as described previously[35]. The entire stroke-affected hemisphere was imaged using fluorescent microscopy[36]. Perfused collaterals were quantified from FITC-lectin labeled vessels and expressed as percent area of the entire hemisphere. Total blood vessels in the stroke-affected hemisphere were quantified from all CD31 labeled blood vessels.

Laser Microdissection Pressure Catapulting and RNA isolation. For laser capture microdissection, OCT-embedded brain tissue was sliced into 12μm thick sections using a cryostat. Sections were mounted onto RNase inhibitor-treated thermoplastic (polyethylene napthalate)-covered glass slides (PALM Technologies, Bernried, Germany). In this work we refer to collaterals as FITC-lectin perfused vessels isolated from stroke-affected primary somatosensory (S1) cortex. FITC-lectin labeled collaterals from the stroke-affected primary somatosensory cortex were collected using a PALM MicroLaser, MicroBeam, and RoboStage/RoboMover system (**Figure 10**). More than 150,000μm^2 of capture elements were collected (**Table 3**) for downstream RNA isolation, cDNA synthesis and real-time PCR. After laser cutting, the isolated collaterals were catapulted directly into 35μl of RNA extraction buffer (PicoPure RNA Isolation kit;

Life Technologies, Grand Island, NY, USA) situated directly above the section in a microtube cap. An additional 15µl of extraction buffer was added after collection. RNA was isolated from captured and catapulted elements using the PicoPure RNA Isolation Kit as described[37].

Real-Time PCR. Gene expression levels of arteriogenic targets were independently determined at 24 hours from contralateral control and stroke-affected laser microdissection pressure catapulting-captured elements using real-time PCR, as previously described[37]. Total RNA was reverse transcribed into cDNA using oligo-dT primer and Superscript III (Life Technologies, Grand Island, NY, USA). Reverse transcriptase-generated DNA was quantified by real-time PCR assay using double stranded DNA-binding dye SYBR Green-I (Life Technologies, Grand Island, NY, USA) with custom made primers (Integrated DNA Technologies, Coralville, Iowa, USA). All primer sequences have been provided (**Table 4**).

Statistical Analysis. Statistical analysis of data was performed using Microsoft Excel software (v12.3.6). All data are reported as mean ± standard deviation. Difference between means was tested using Student's *t*-test ($p<0.05$).

A timeline is provided to clarify the chronological steps of the study (**Figure 11**).

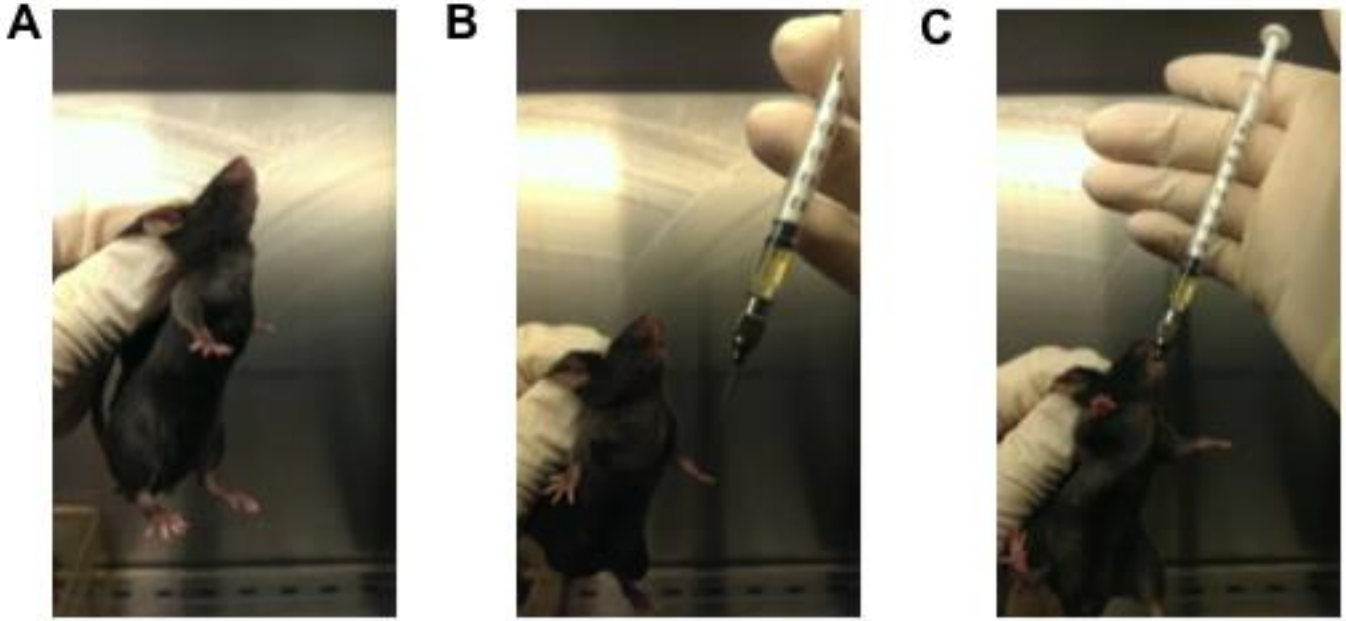

Figure 5. Vitamin E supplementation of mice via oral gavage. Mice gavaged for 4 or 6 week duration, with a dosage of 50 mg/kg body weight. (**A**) Shows the mouse being held in preparation for gavaging. (**B**) The gavaging syringe is loaded with Vit E, and the gavaging needle is shown. (**C**) The completed process of inserting the needle into the stomach is shown here. The syringe contents are then emptied into the stomach and the process completed.

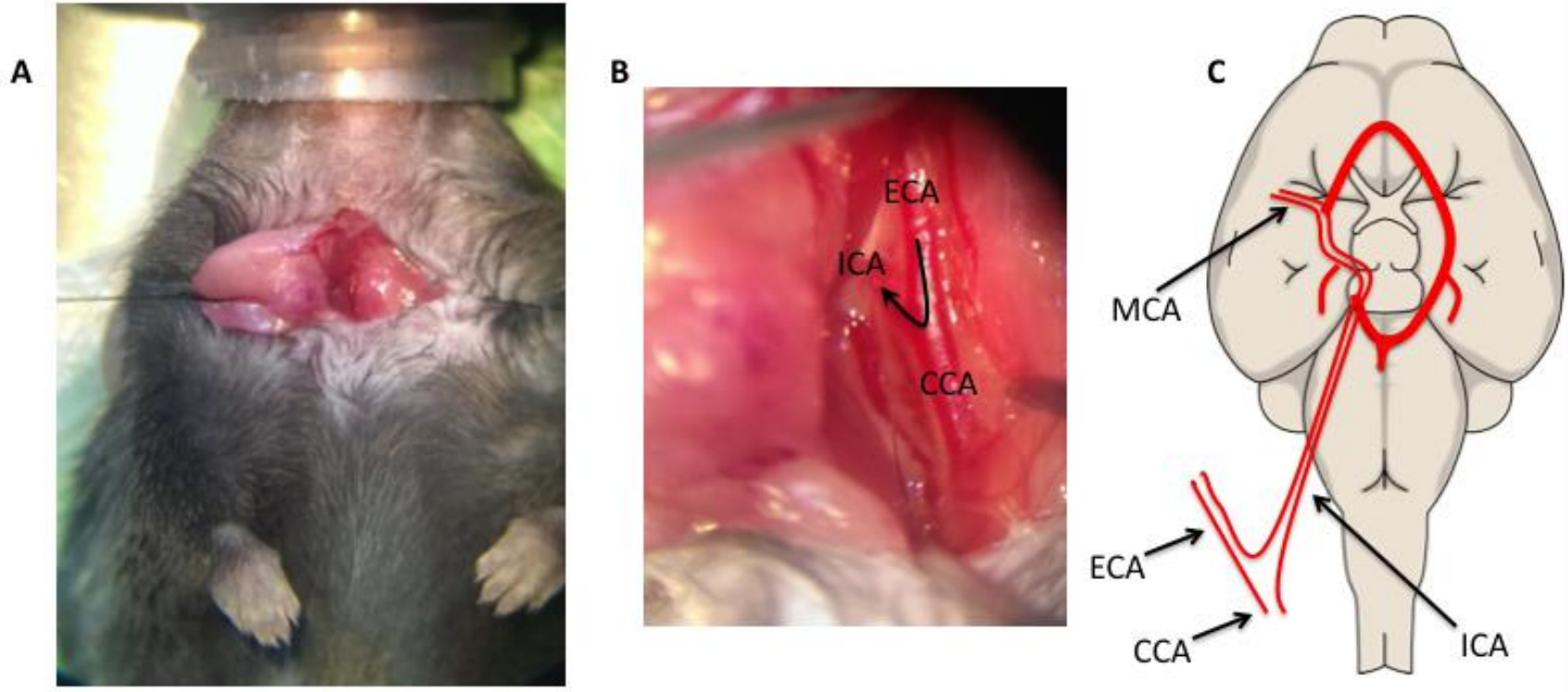

Figure 6. Surgical model for ischemic stroke in mice. Surgical model of MCAO, showing the placement of the ischemia, and how we can produce this surgically. **(A)** 1.5cm ventral midline incision on the neck of the mouse allows for access to the common carotid artery. **(B)** Surgical field as seen through stereoscope. The bifurcation seen here is the external common carotid and the internal common carotid. The suture with occluder tip (as drawn in over the vessel) is passed from the ligated external carotid artery into the internal carotid approximately 8mm until reaching the origin of the middle cerebral artery.

Reagent Volume for Vitamin E Extraction							
Sample ID	Wet Tissue Weight (mg)	PBS (ml)	SDS (ml)	BHT (ul)	Ethanol (ml)	Hexane (ml)	Amount Hexane recovered (ml)
PBO-1	116	1.16	1.16	58.0	2.32	2.32	1.740
PBO-2	165	1.65	1.65	82.5	3.30	3.30	2.475
PBO-3	126	1.26	1.26	63.0	2.52	2.52	1.890
PBO-4	107	1.07	1.07	53.5	2.14	2.14	1.605
PBO-5	118	1.18	1.18	59.0	2.36	2.36	1.770
PBO-6	103	1.03	1.03	51.5	2.06	2.06	1.545
TCT-7	183	1.83	1.83	91.5	3.66	3.66	2.745
TCT-8	118	1.18	1.18	59.0	2.36	2.36	1.770
TCT-9	133	1.33	1.33	66.5	2.66	2.66	1.995
TCT-10	118	1.18	1.18	59.0	2.36	2.36	1.770
TCT-11	155	1.55	1.55	77.5	3.10	3.10	2.325
TCT-12	154	1.54	1.54	77.0	3.08	3.08	2.310

Table 2. Vitamin E Extraction Table. The table shows the ground brain tissue sample weight and calculated reagent amounts used for vitamin E extraction. This calculation table uses the tissue weight to calculate the necessary amount of PBS, SDS, BHT, ethanol, and hexane to be added to the homogenized tissue for the extraction process. Once this is completed, the hexane is recovered, which contains the vitamin E extracted from the tissue. This extracted product was then used for HPLC quantification of vitamin E.

Line #	Time (min)	Activity	Value
1	0.00	FLOW	0 %B 0.60 ml/min
2	0.00	AUTOSAMPLER INJ	1.0 Sec
3	0.00	WAIT EXTERNAL	START 1
4	0.00	FILE	START
5	0.50	AUTO ZERO	ON
6	6.00	FLOW	85 %B 0.60 ml/min
7	12.00	FLOW	100 %B 0.60 ml/min
8	14.00	CLEAN CELL	ON: 0,0,0,0,0,0,0,0 mV
9	15.00	CLEAN CELL	OFF
10	16.00	FILE	STOP
11	16.00	FLOW	0 %B 0.60 ml/min

Figure 7. HPLC Data Acquisition Method. Acquisition method as seen on the computer, programmed through CoulArray software. Shows the individual time points and steps taken during a normal run on HPLC to simultaneously detect multiple vitamin E isomers.

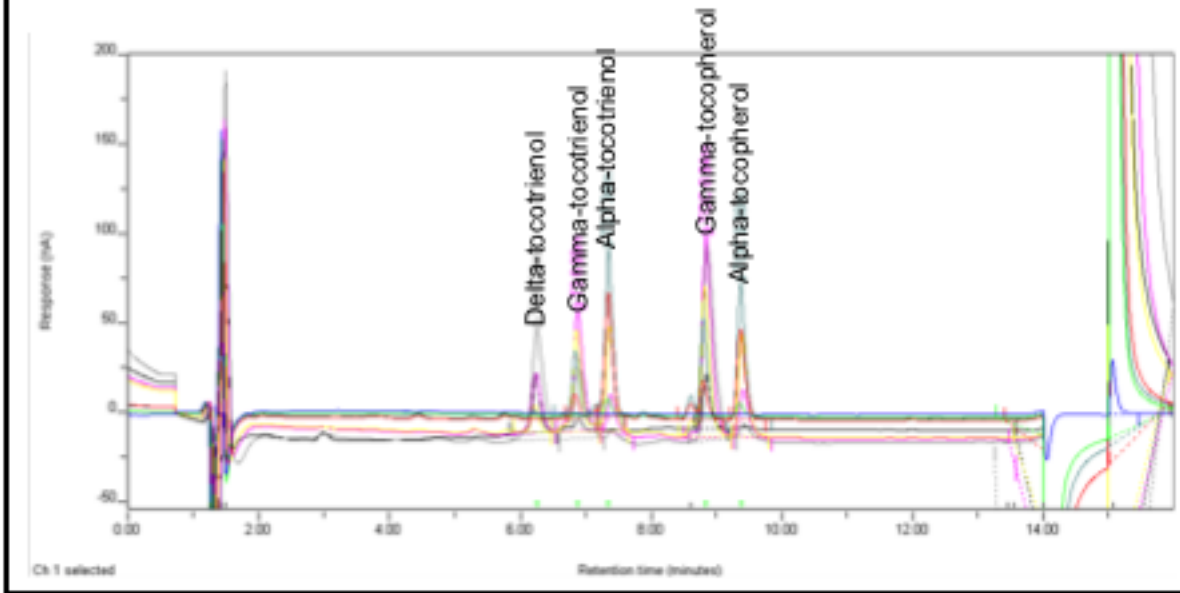

Figure 8. HPLC Chromatograph. Representative chromatogram from 1μM standard on HPLC machine to verify detection. Shows detection of all five vitamin E isomers present in the standard including; delta-tocotrienol, gamma-tocotrienol, alpha-tocotrienol, gamma-tocopherol, and alpha-tocopherol.

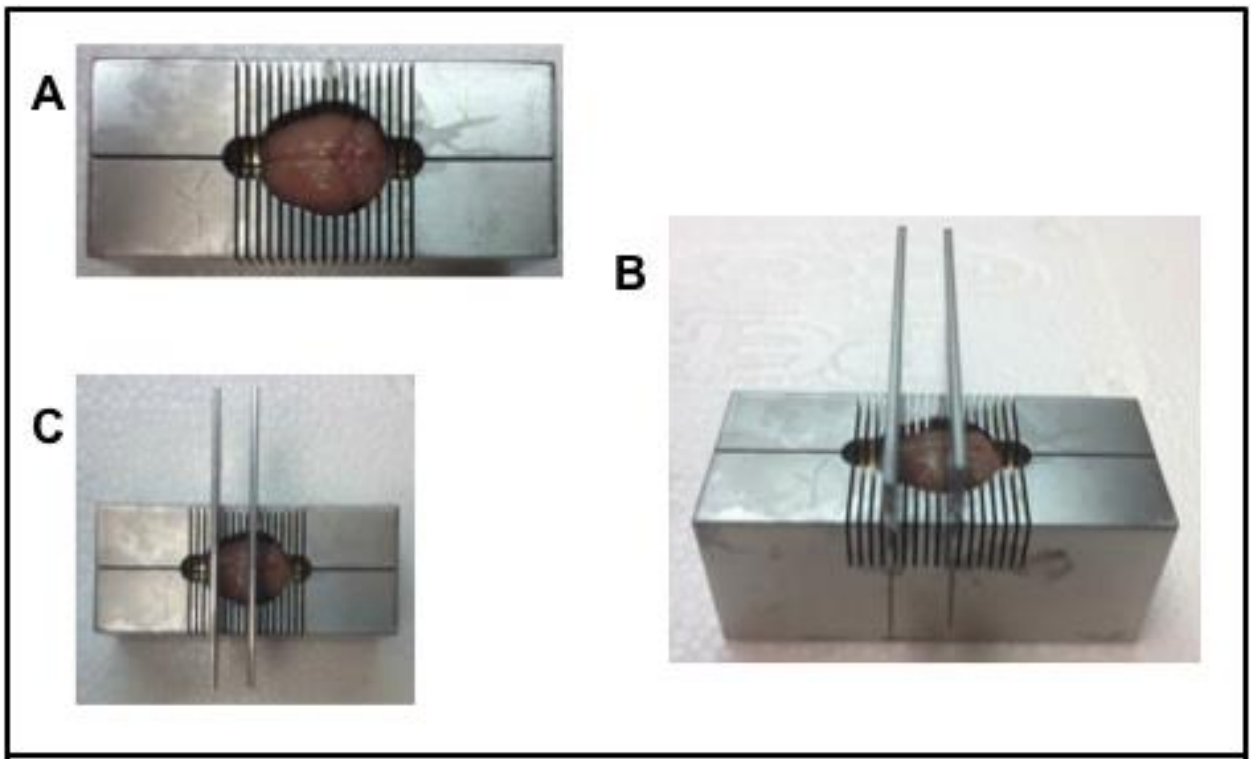

Figure 9. Embedding mouse brain for downstream sectioning and laser capture microdissection. We target collection of the primary somatosensory (S1) cortex, which is supplied by the middle cerebral artery. (**A**) Shows the brain properly mounted into the brain matrix. (**B**,**C**) Two different views of how the brain matrix in conjunction with razor blades is used to slice the brain tissue. The first blade is placed at bregma +3.08mm, and the second blade placed at bregma -2.30mm.

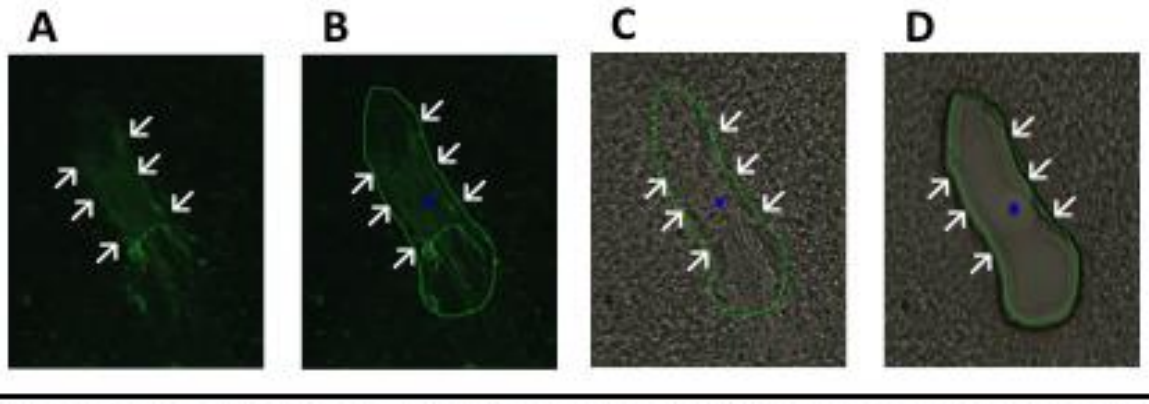

Figure 10. Laser Capture Microdissection of FITC-lectin perfused vessels in the brain. Vessels were selectively captured from contralateral control and ipsilateral stroke-affected cerebral cortex after stroke onset. Using FITC-lectin fluorescence, vessels were differentiated from other brain tissue. **(A)** Shows FICT-lectin perfused vessel under florescence on LCM microscope. **(B)** Selection of vessel for capture under florescence. **(C)** Selected vessel as seen through microscope without florescence. **(D)** View of tissue post capture.

Sample ID	Stroke-Collected area (μm²)	Control-Collected area (μm²)
PBO-1	177,000	186,000
PBO-2	175,000	187,000
PBO-3	182,000	199,000
PBO-4	174,000	176,000
PBO-5	173,000	181,000
PBO-6	161,000	182,000
Average (±SD)	173,667 (±6,976)	185,167 (±7,834)
TCT-7	185,000	181,000
TCT-8	179,000	180,000
TCT-9	179,000	186,000
TCT-10	174,000	207,000
TCT-11	201,000	181,000
TCT-12	176,000	187,000
Average (±SD)	182,333 (±9,873)	187,000 (±10,218)

Table 3. Laser Capture Microdissection Collection Yield. The table shows the amount of tissue collected for each specific sample using the laser capture technique for endothelial specific collection. Tissue was collected from the S1 cortex within the stroke affected hemisphere, or from the non-stroke affected region.

Primer ID	Primer Sequence
VWF	F: 5'-CCGGAAGCGACCCTCAGA-3'
	R: 5'-CGGTCAATTTTGCCAAAGATCT-3'
NF-H	F: 5'-CGAGCTGTACGAGCGCGAGG-3'
	R: 5'-AGCTCGCCCACCTCCTCCTG-3'
GFAP	F: 5'-CACGTGGAGATGGATGTGGC-3'
	R: 5'-CAGTTGGCGGCGATAGTCATTA-3'
TIMP1	F: 5'-GTGCTGGCTGTGGGGTGTGC-3'
	R: 5'-GCCTGGATTCCGTGGCAGGC-3'
TIMP2	F: 5'-TGCTGCTAGCCACGCTGCTG-3'
	R: 5'-CGAGACCCCGCACACTGCTG-3'
MMP2	F: 5'-CCAGGACCTGCAAGCACCCG-3'
	R: 5'-TGATGGGCGATGGTGCAGCG-3'
MMP9	F: 5'-GGCCTTCTGGCACACGCCTT-3'
	R: 5'-GCCTTCTCCGTTGCCGTGCT-3'
KLF2	F: 5'-CTTTCGCCAGCCCGTGCCGCG-3'
	R: 5'-AAGTCCAGCACGCTGTTGAGG-3'
DLL1	F: 5'-GACACCAAGTACCAGTCGGTGTATG-3'
	R: 5'-AACCTGGTTCTCAGCAGCAGTC-3'
DLL4	F: 5'-CGGGTCATCTGCAGTGACAAC-3'
	R: 5'-AGTTGAGATCTTGGTCACAAAACAG-3'
EphrinB2	F: 5'-GCGGGATCCAGGAGATCCCCACTTGGACT-3'
	R: 5'-GTGCGCAACCTTCTCCTAAG-3'
PCAF	F: 5'-TCATGCTCCCGAGGAGGCCA-3'
	R: 5'-CCCCTGCGTTCTTCCAGCCG-3'
CD44v3	F: 5'-TCTGGATCAGGCATTGATGA-3'
	R: 5'-CGCAGTTGAGTGTCCAGCTA-3'
CLIC1	F: 5'-GCTGGCTGCCCTGAACCCTG-3'
	R: 5'-GCCCTCATCTTCGGCGCTGG-3'
CLIC4	F: 5'-TGCCCCTGCAGTGTCTCCGT-3'
	R: 5'-TCGTGGGCACCTCACACCCA-3'

Table 4. Primer Sequences. The table shows sequence of all the primers used throughout the study, with both forward (F) and reverse (R) sequences. Not shown are the 18s rRNA primers, which was run using the Life Technologies TaqMan® kit and the primers provided.

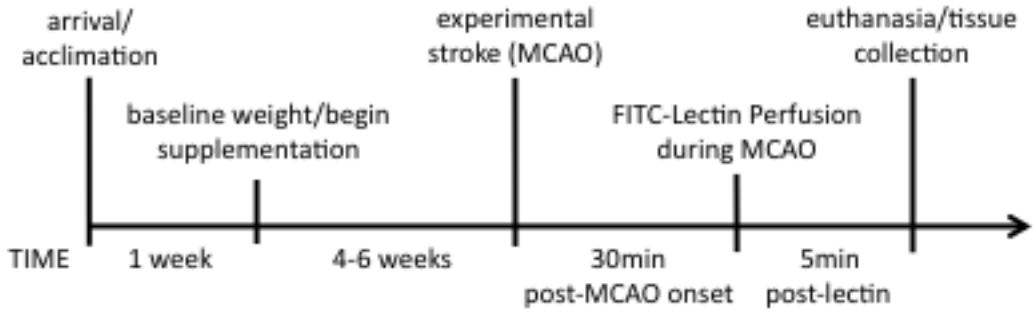

Downstream Analyses
(in chronological order)

1. HPLC determination of vitamin E content
2. IHC quant. of collaterals
3. Sectioning/Laser capture
4. RNA isolation from laser capture material
5. cDNA synthesis and RT-PCR

Fig. 11. Experimental timeline (not to scale). The timeline gives a better appreciation for the process and order of steps taken throughout the methodology of the project. First animals were given 1 week to acclimate to their new environment before gavaging started. Oral gavaging with TCT or placebo persisted for 4 to 6 weeks depending on the subject. Once supplementation was completed, surgical stroke was induced using the intraluminal MCAO method. The mice were occluded for 30 minutes before being perfused with FITC-conjugated lectin, while occlusion still persisted. The lectin was given 5 minutes to circulate before euthanization of the mouse. Once euthanized the brain tissue was collected and processed, allowing for downstream molecular analyses.

Results:

Verification of results in a rodent model. Informed by our canine study, we repeated 10 week supplementation studies in mice to specifically look at cerebral blood flow in the brain during ischemic stroke. As in canine, 10 week prophylactic supplementation of TCT in mice significantly attenuated stroke induced lesion volume (**Figure 12**). Collateral blood flow was studied in these mice using laser speckle flowmetry imaging. Results show that 10 week TCT supplementation is successful at increasing cerebral blood flow to the stroke-affected region (**Figure 13**). On the basis of these outcomes, the current work was designed to test expression of pro-arteriogenic factors at earlier time points (4-6 weeks) to determine whether the TCT-mediated change in arteriogenesis was an acute response (at the time of MCAO) or the result of chronic changes over the course of supplementation.

Brain vitamin E levels following prophylactic TCT supplementation. Given the natural variation in mouse development and body weight, mice were weighed weekly and TCT gavage dose was adjusted accordingly to achieve a concentration of 50mg/kg body weight. To account for variability in the amount of brain tissue collected at euthanasia, vitamin E content was normalized to brain protein content (pmol vit E/mg protein). Protein quantification was performed using the bicinchoninic acid assay (BCA, **Figure 14**). The BCA protein assay is a biochemical assay used to determine total protein concentration. The assay is colorimetric, meaning it relies on the detection of light absorbance at 562nm in order to determine protein concentration by comparison to

a standard. This technique was used to determine brain tissue protein content for each mouse. Subsequently, vitamin E levels determined by HPLC were normalized to brain protein concentration. **Figure 15** demonstrates that TCT supplementation enriched brain tissue with α-tocotrienol by 12.09 nmol/g protein. The murine diet provided is deficient in all tocotrienols, resulting in the detection of no significant amount of tocotrienol in brain tissue of the PBO controls using HPLC-coulometric electrode array detection. Of note, the concentration of brain α-tocotrienol in TCT-supplemented animals was 12.3 times less than that of α-tocopherol in the cerebellum, which represents the most bioavailable vitamin E isoform found in the body (**Figure 15**). This outcome is in line with known uptake mechanisms for alpha-tocopherol by the tocopherol transfer protein (TTP), which has an 8.5-fold greater affinity for tocopherols versus tocotrienols[38], though this may vary based upon tissue type[39,40]. TCT supplementation also modestly increased the concentration of α-tocopherol in brain tissue as compared with PBO controls. Our TCT supplement, while highly enriched with alpha-tocotrienol, is only 70% pure, the remainder of which contains other vitamin E isoforms, including alpha-tocopherol. Taken together, results demonstrate that mice orally supplemented with TCT for only 4-6 weeks significantly increased the concentration of tocotrienols in the brain as compared to PBO controls.

Tocotrienol supplementation increases collateral perfusion during acute ischemic stroke. Our recently published observation[31] that prophylactic TCT supplementation improved cerebrovascular collateral circulation during stroke uncovered new putative mechanisms for TCT protection against stroke injury. This observation was enabled by

a large animal (canine) endovascular stroke model that employed real-time cerebral angiograms for documentation of cerebral perfusion during stroke. The canine study revealed, through the retrospective study of angiograms, that collateral blood flow had improved in the TCT supplemented canines. Angiograms revealed improved collateral blood flow, allowing for retrograde filling of occluded parent vessels through anastomosing collaterals (**Figure 16**). To confirm results, a physician was shown the angiograms to objectively assess the collateral blood flow seen in each subject on an 11-point scale of the stroke-affected hemisphere. The physician, blind to the study, gave significantly higher scores to the supplemented group when compared to the placebo. This increased collateral blood flow is thought to be the reason for decreased infarct volumes seen within the canine study. Until this work, TCT had been described to attenuate stroke-induced injury on the basis of neuroprotection alone[29]. In light of cost, molecular reagent availability, and low-throughput surgeries associated with the canine stroke model, we sought to develop tools to test mechanistic hypotheses of TCT-induced arteriogenesis in a small animal (murine) stroke model. To visualize cerebral perfusion in mouse during MCAO, fluoroscopic angiograms are not a viable option. We therefore developed the following immunohistochemical approach to visualize cerebral perfusion during acute ischemic stroke. During ischemia, mice were injected with FITC-conjugated lectin, sections of the same brain were also immunostained using CD31, a marker of endothelial cells[41]. This lectin compound, a carbohydrate binding protein aiding in molecular recognition specific to sugar moieties, is derived from tomato. The name lectin itself is derived from the Latin term *legere,* which means “to select”. The particular lectin used here binds selectively to perfused endothelial cells, allowing

visualization of structures in the microvasculature when viewed by fluorescent microscopy, refer to **Figure 10**. To stain all endothelial cells in brain tissue, regardless of perfusion, we employed CD31 immunostaining. CD31 is an immunoglobulin superfamily member. As an immonglobulin, CD31 mediates adhesion and trans-endothelial migration of T-lymphocytes into the vascular wall, as well as T cell activation and angiogenesis. CD31 is localized on the surface of endothelial cells[42]. Using these two staining methods in combination allows for relative quantification of total vasculature and perfused vasculature during ischemia (**Figure 17**). These images are then compared and merged in order to show the change in perfused collateral blood flow of the stroke-affected region of the brain, but not an overall increase in number of total blood vessels present in the brain, lending credence to the process of arteriogenesis. Quantification showed that prophylactic TCT supplementation significantly increased lectin perfusion in the S1 cortex by 2.3 fold (p=0.01) following 4+ weeks supplementation.

Endothelial cell specific laser capture microdissection (LCM) from brain tissue. A major obstacle with studying brain vasculature is the contamination of other cell types in collected tissue, such as neuron or glial cells. To avoid such contamination in collected tissue samples, a technique known as laser capture microdissection (LCM) was employed that enables site and cell specific resolution of tissue biology. This approach allowed for selective capture of blood vessels from brain tissue using an LCM microscope guided by FITC-lectin tagged endothelial cells of perfused vessels. Laser captured collection yield (**Table 3**) shows the area of collected tissue from each

samples, separating the stroke affected and contralateral sides for separate analyses. With these tissue samples collected, RNA isolation was then performed using the PicoPure RNA Isolation kit (Arcturus, Mountain View, CA, USA). Initial analysis of the RNA was determined using a NanoDrop spectrophotometer (NanoDrop Technologies, Wilmington, DE). The machine provided nucleic acid concentrations, as well as purity information in the form of 260/280 and 260/230 ratios to determine protein or other contaminants presence in the sample (**Table 5**). The ratio of 260/280 gives the absorption found at 260nm light and 280nm. The nucleic acids absorb light best at 260nm, while proteins and phenols, which are commonly used in RNA extraction, absorb light strongly at 280nm. The same principles hold true for the 260/230 ratio, as thiocynates, carbohydrates, some phenols, and other organic compounds best absorb light at 230. While an acceptable 260/280 ratio is between 1.8-2.0, our values were consistent with the collection range for laser capture microdissection of ~1.5[31].

Screening for TCT sensitive arteriogenic markers. Arteriogenesis refers to a positive outward remodeling of pre-existing collateral arteries into larger vessels, which are able to circumvent sites of occlusion and perfuse otherwise stroke-affected tissue[33,43]. To determine whether TCT supplementation invoked molecular mechanisms of cerebral arteriogenesis at an earlier (4-6 week) time point, endothelial cells from the stroke-affected and contralateral control cerebral cortex were selectively isolated and prepared for PCR analysis. With prepared tissue, PCR analysis was used to confirm collection of endothelial cells, using von Willebrand factor (vWF) as a endothelial cell marker, glial fibrillary acidic protein (GFAP) as a glial cell marker, and neurofilament heavy

polypeptide (NFH) as a marker for neurons[8] (**Figure 18**). Of interest were multiple markers previously indicated to play a key role in the process of arteriogenesis[44]. Previously identified markers includes; matrix metalloproteinase family members (MMP2, MMP9), tissue inhibitor of metalloproteinase family members (TIMP1, TIMP2), chloride intracellular channel family members (CLIC1, CLIC4), Krüppel-like Factor 2 (KLF2), cluster of differentiation variant 3 (CD44v3), P300/CBP-association factor (PCAF), and Shc1 sensitive targets (EphrinB2 and delta-like 1 and delta-like 4). For quick reference of arteriogenic targets, refer to **Table 1**.

Matrix metalloproteinases (MMP) 2 and 9 have previously been identified as key contributors within the process of arteriogenesis[44]. MMPs are a family of zinc-dependent endopeptidases which are able to break down extracellular matrix[45]. MMP2 and MMP9 belong to a class of MMPs known as gelatinases, which are unique from the other MMPs in their role as proteolytic enzymes. This class is capable of breaking down gelatin and type IV collagen found in the basal lamina, a layer of extracellular matrix secreted by the endothelial cells. Due to this activity, the role of gelatinases is critical for the remodeling of vessels. Our data shows this family is responsive to TCT supplementation, with MMP2 mRNA being down-regulated significantly (2.46x decrease, p=0.002, **Figure 19**), and MMP9 showing a trend towards down-regulation as well (2.51x decrease, p=0.68, **Figure 20**), though the results were not statistically significant.

Of specific interest during our project were TIMP1 and TIMP2, for their previously identified roles as inhibitors of MMPs, aiding in the process of collateral remodeling via arteriogenesis[33]. These genes and their products fall within a family known as tissue inhibitor of metalloproteinase (TIMP). This family of genes encode for proteins of the same name, which are natural inhibitors of the matrix metalloproteinases (MMPs). TIMP1 and TIMP2 were chosen for study, as they are known inhibitors of MMP2 and MMP9. With their ability to function as inhibitors of these MMP peptidases, the TIMP family is known to play an important role as the regulator of MMPs in the brain. Previous work has shown that TIMP1 gene regulation is responsive to TCT supplementation[31]. Our findings here report a down-regulation of TIMP1 in the collected tissue samples (2.49x decrease, p=0.01, **Figure 21**), which confirm sensitivity to supplementation, while TIMP2 was not significantly affected (1.67x increase, p=0.17, **Figure 22**).

Previous work identified chloride intracellular channel (CLIC) 1 and 4 to be up regulated by supplementation of TCT[31]. These CLICs belong to a group of genes and their protein products that regulate processes including stabilization of cell membrane potential, transport across the epithelium, cell division, apoptosis, and cell motility[46,47]. The CLIC proteins are thought to influence the process of arteriogenesis by acting upstream of other genes relevant for vascular growth, including hypoxia-inducible factor-1α, vascular endothelial growth factor-A (VEGF-A), and angiopoietin-2[48]. CLIC1 and CLIC4 have been shown to be sensitive to TCT supplementation[31]. The CLIC family is also known to play an important role in the process of cell hallowing and widening, known as tubulogenesis, which is critical for functional arteriogenesis[49,50]. Data collected in this

study showed no changes in mRNA expression of either CLIC1 (1.67x decrease, *p*=0.22, **Figure 23**) or CLIC4 (1.58x increase, *p*=0.20, **Figure 24**) markers at the earlier 4-6 time point for collection.

Krüppel-like Factor 2 is a newly identified arteriogenic marker[51], it is understood to be induced by shear-stress, resulting from laminar flow of blood through the vascular tissue. The increased gene expression within the endothelial cells leads to anti-inflammatory response due to inhibiting activation of p65, anti-thrombolytic effect caused by up-regulation of endothelial nitric oxide synthase and thrombomodulin, and anti-angiogenesis properties via inhibition of vascular endothelial growth factor (VEGF) receptor 2[52]. It is understood to be crucial in vascular development, with previous research showing that knockout mice die around embryonic day 13 due to severe embryonic hemorrhaging[53,54], and thus is thought to be critical in vessel development and integrity throughout life. Importantly, this work is the first to determine whether KLF2 mRNA expression is TCT sensitive. Results of this study have shown that TCT supplementation causes a trend of moderate down-regulation in KLF2 that is very close to statistical significance (3.29x decrease, *p*=0.08, **Figure 25**). We hypothesize that this down-regulation would be significant if supplementation persisted to the 10 week time point. Statistical significance may be reached at the 4-6 week time point if the study were better powered.

Previous work has indicated that during the process of arteriogenesis, both total CD44

as well as CD44 variant 3 (CD44v3) are up regulated and result in improved arteriogenic outcomes[55]. The gene encodes for a cell-surface glycoprotein, specifically involved in cell-to-cell interactions, cell adhesion and migration. The protein functions as a receptor to hyaluronic acid and other ligands, such as osteopontin, collagens, and MMPs. This interaction with the MMP family is hypothesized as the connection between these surface proteins and the process of arteriogenesis. CD44v3 is one of many variants that arise from the transcription of this gene as transcripts undergo complex alternative splicing that results in many functionally distinct isoforms[56]. This glycoprotein has not been studied in previous TCT supplementation projects, and as such the gene's sensitivity to TCT was unknown. Though screened here, no data resulted from the testing (**Figure 26**). We conclude that expression was either very low, or that amplification did not result due to poor primer design. Further testing with new primer design is required.

K (lysine) acetyltransferase 2B (KAT2B), also known as P300/CBP-associated factor (PCAF), is a transcriptional co-activator associated with the p53 protein. This protein has recently been indicated as playing a large role in arteriogenesis[57]. PCAF has histone acetylating activity and promotes transcription of multiple inflammatory genes. As arteriogenesis is an inflammatory driven process, PCAF is seen as a multi-factorial regulator of this process through its regulation of inflammation. To confirm, recent studies have shown that in mice, PCAF deficiency reduced the *in vitro* inflammatory response in leukocytes and vascular cells involved in arteriogenesis interrupting the process significantly. We had not previously study this gene, so it's sensitivity to

supplementation is unknown. Results showed no alteration in the expression of PCAF mRNA within the samples (p=0.86, **Figure 27**).

Shc1 is a gene that holds an important function in the process of arteriogenesis. The gene is activated by the onset of shear stress and integral in two pathways necessary for the arteriogenic process to be successful[58]. Shc1 knockout mice have impaired activation of the nuclear factor κ-light-chain-enhancer of activated B-cell (NF-κB)-dependent inflammatory pathway[59]. Additionally, Shc1 is required for shear-stress mediated arteriogenic remodeling and induces up-regulation of the endothelial cell marker ephrinB2 and activation of the Notch pathway by ligands delta-like 1 (DLL1) and delta-like 4 (DLL4). To test whether targets of the Shc1 pathway were sensitive to TCT supplementation, we assessed gene expression of EphrinB2, DLL1, and DLL4. EphrinB2 is a target gene of the notch pathways, and was studied to identify a change in notch pathway activity. EphrinB2 was shown to significantly decrease in mRNA expression due to TCT supplementation (1.72x decrease, p=0.01, **Figure 28**). To further this pathway, ligands of the notch pathway were also analyzed. These ligands include delta-like 1 and delta-like 4. In these ligands, we saw no significant change and an increase respectively. Results show delta-like 1 change being statistically insignificant (6.44x increase, p=0.19, **Figure 29**), while delta-like 4 was significant (3.96x increase, p=0.04, **Figure 30**). The genetic markers studied here have all been consolidated into a schematic diagram to better represent their role in the process of arteriogenesis (**Figure 31**).

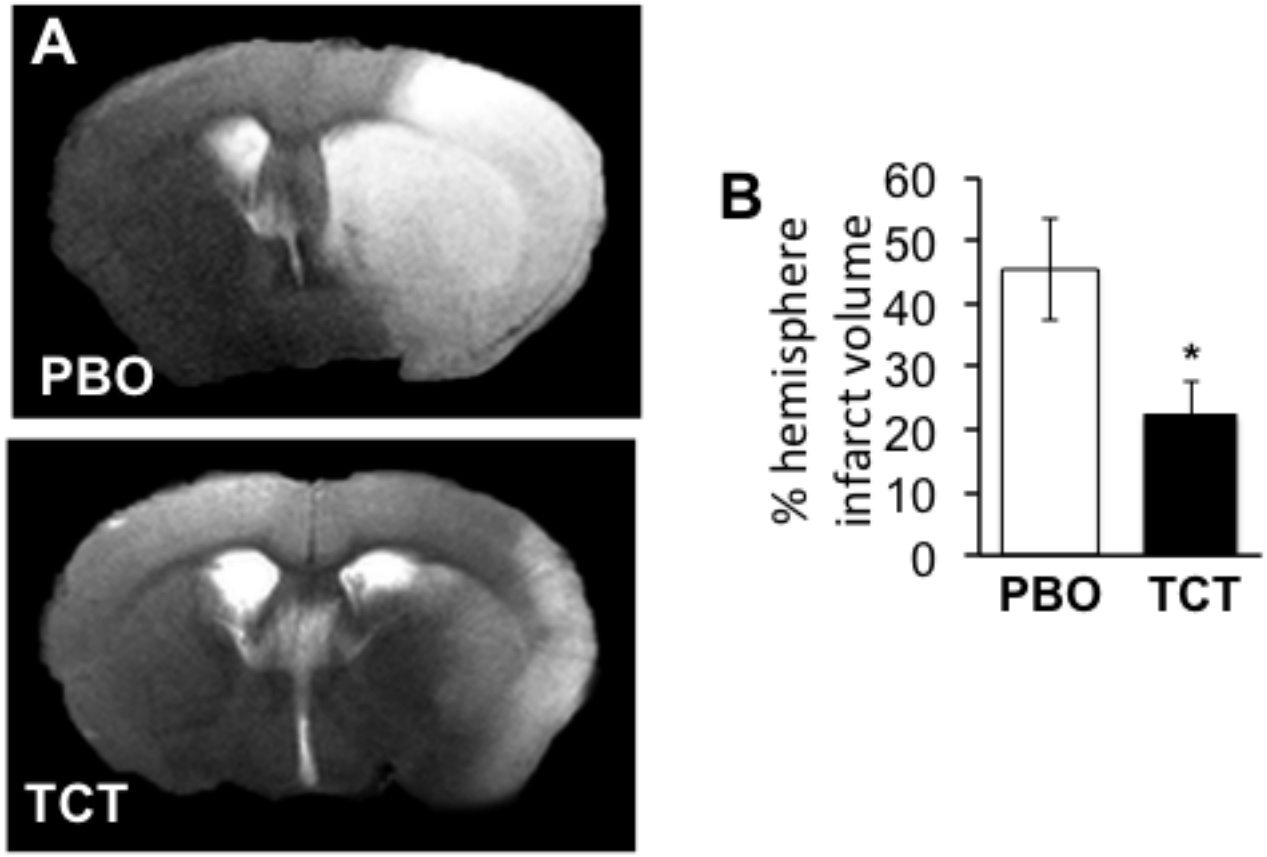

Figure 12. Oral TCT is delivered to brain tissue and attenuates acute ischemic stroke-induced lesion volume. (A) 48h after MCAO, stroke-induced lesion volume was determined by 11.7T MRI and (**B**) quantified by digital planimetry. TCT supplementation of 10 weeks significantly lowered stroke-induced brain lesion volume as compared to PBO control. Data courtesy of Mallory Heigel and Surya Gnyawali.

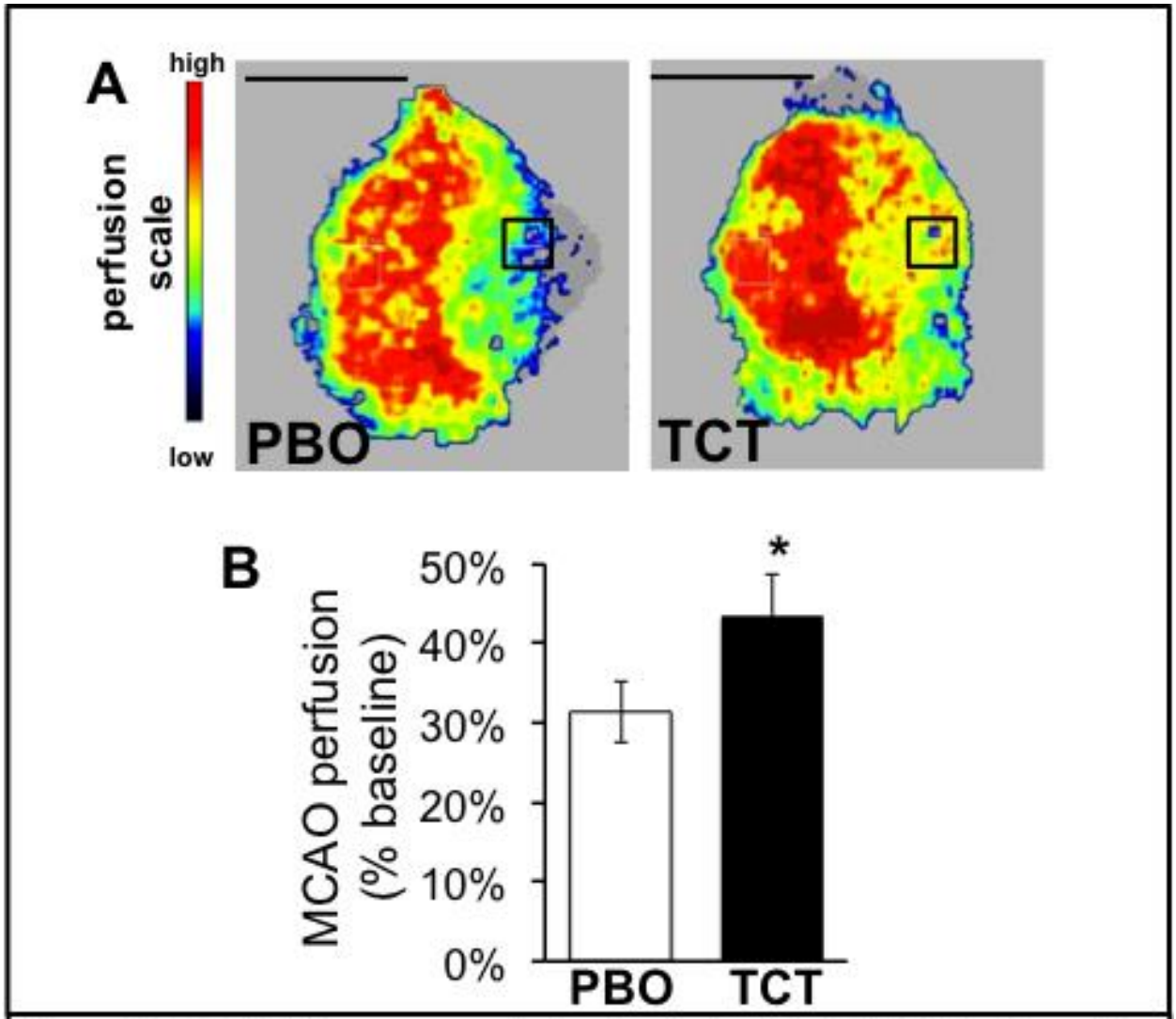

Figure 13. Oral TCT improves perfusion in stroke-affected MCA territory. Mice were supplemented with PBO (vehicle) or TCT (50mg/kg) for 10 weeks prior to MCAO. Real-time, non-invasive, cerebrovascular perfusion imaging of the dorsal surface of the brain was acquired in mice at baseline (not shown) and (**A**) during MCAO-induced acute ischemic stroke using PeriScan™ PSI laser speckle flowmetry; bar = 5mm. TCT mice had significantly higher perfusion in stroke-affected MCA (black box ROI) as compared to PBO controls. (**B**) Perfusion quantified from perfusion units as a percent of baseline. Data courtesy of Mallory Heigel and Surya Gnyawali.

A

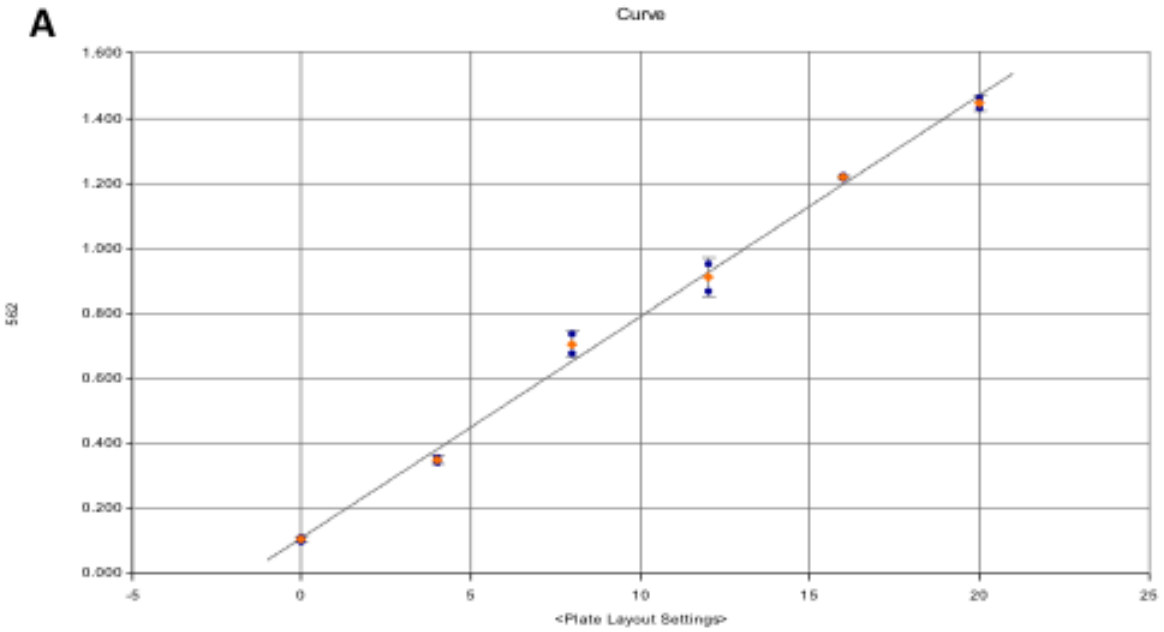

B

Standard Curve Fit			
Curve Formula	**A**	**B**	**R²**
Y=A*X+B	0.068	0.109	0.996

C

ID	Protein (µg/µL)
PBO1	2.84
PBO2	2.47
PBO3	3.04
PBO4	2.87
PBO5	2.87
PBO6	2.90
TCT7	2.99
TCT8	3.37
TCT9	2.59
TCT10	3.00
TCT11	3.94
TCT12	3.60

Figure 14. Protein quantification of brain tissue. BCA Protein Assay was used for protein quantification. **(A)** Standard curve produced by BCA Assay run. To create this, the machine analyzes the color change (using colorimetric techniques) shown in a standard gradient, then produces the standard curve seen here. To find protein quantity in unknown samples are compared, using color change, to the standard. **(B)** To ensure successful BCA protein assay results, the experimental concentrations found are plotted on the same graph as the standard curve, to ensure a the data fits tightly to the curve create by the standards. **(C)** Resulting protein quantification is seen here. Given values show micrograms of protein per microliter of blood.

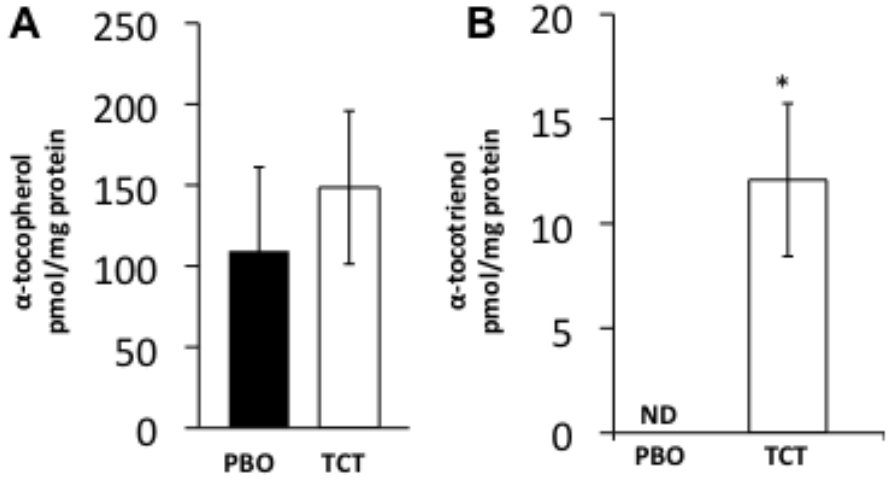

Figure 15. Oral alpha-tocotrienol (TCT) is delivered to brain tissue. Results of 4 to 6 week oral supplementation on cerebral cortex concentrations of α-tocopherol (**A**) and α-tocotrienol (**B**). A moderate, but insignificant increase in brain α -tocopherol level was observed as TCT gavaging contained 10% α-tocopherol w/v. (**B**) No α-tocotrienol was detected in brain of PBO supplemented mice. TCT gavaging for 4-6 weeks significantly increased brain α-tocotrienol levels.

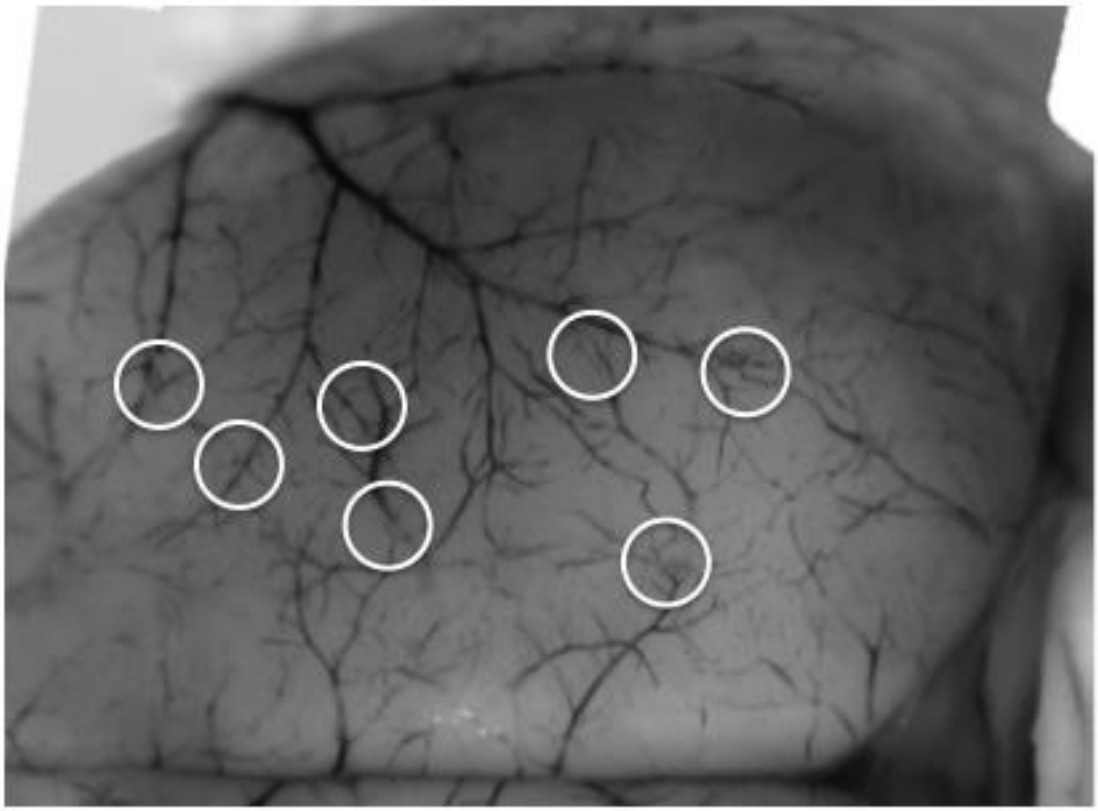

Figure 16. Collateral blood flow of anastomosing vessels in the brain. Shows the mouse brain vasculature. The black coloration, due to injecting an acrylic resin, allows for visualization of the superficial vessels of the brain lie. From this picture it is possible to see the group of vessels that anastomose and are therefore capable of retrogradely supplying blood to the parent vessel in the case of ischemia.

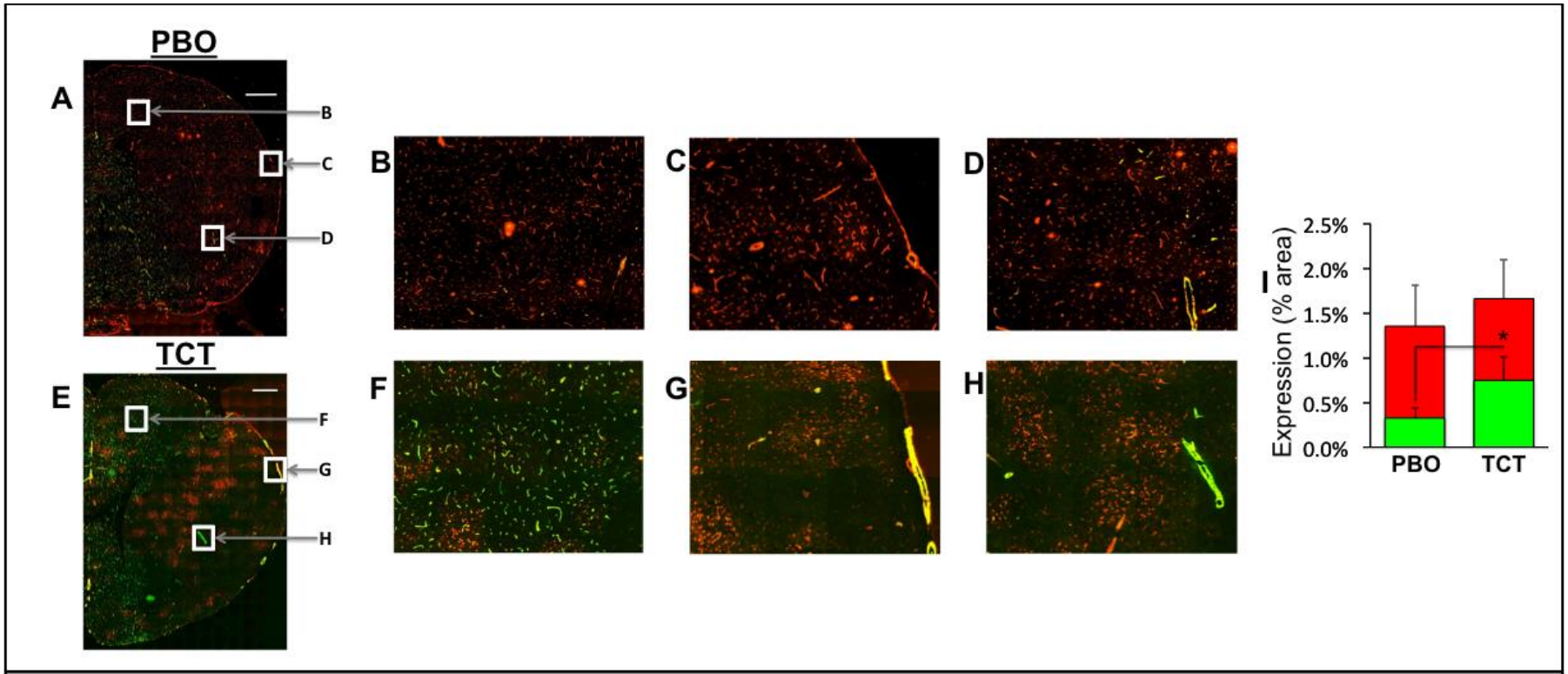

Figure 17. Immunohistochemical staining of brain tissue for endothelial quantification. Following 4wks of oral supplementation, PBO and TCT mice were subjected to MCAO. After 30min of stroke, and while ischemia persisted, mice were perfused with FITC-conjugated lectin (green) to visualize perfused vessels of the stroke-affected S1 cortex. Further immunohistochemical staining was performed for visualization of total vasculature. **(A,E)** Representative S1 cortex depicting FITC-lectin perfused collaterals and CD31-immunostained endothelial cells (red) in a merged image for PBO and TCT supplemented mice. **(B-D, F-H)** Areas show FOV regions for comparison between TCT and PBO groups. **(B, F)** representative capillaries from S1 cortex. **(C, G)** Leptomeningeal arterioles. **(D, H)** Striatum arteriole. **(I)** Quantification of immunohistochemical staining shows TCT supplementation significantly increased lectin-positive staining as compared to PBO (*p<0.05) while no difference in CD31 staining (marker for total endothelial cells) was detected.

ID	ng/ul	260/280	260/230
PBO-1 C	14.89	1.50	0.66
PBO-1 S	20.30	1.56	0.49
PBO-2 C	21.27	1.38	0.75
PBO-2 S	10.23	1.39	0.64
PBO-3 C	5.43	1.64	0.31
PBO-3 S	8.21	1.51	0.72
PBO-4 C	29.07	1.45	0.74
PBO-4 S	11.25	1.51	0.74
PBO-5 C	47.53	1.09	1.18
PBO-5 S	14.48	1.58	0.53
PBO-6 C	8.41	1.19	0.07
PBO-6 S	13.51	1.57	0.09
Mean (±SD)	17.05 (±11.65)	1.45 (±0.16)	0.57 (±0.31)
TCT-7 C	22.79	1.50	0.65
TCT-7 S	18.87	1.48	0.71
TCT-8 C	23.01	1.40	0.49
TCT-8 S	5.58	1.62	0.01
TCT-9 C	27.50	1.49	0.67
TCT-9 S	41.97	1.46	0.67
TCT-10 C	22.91	2.55	0.47
TCT-10 S	5.24	1.65	0.85
TCT-11 C	10.48	1.32	0.38
TCT-11 S	7.30	1.65	0.73
TCT-12 C	6.78	1.30	0.83
TCT-12 S	8.12	1.52	0.96
Mean (±SD)	16.71 (±11.40)	1.57 (±0.33)	0.62 (±0.25)

Table 5. RNA Yield and Purity from NanoDrop. The table shows the amount of RNA collected from each sample as determined by NanoDrop. Also shown are 260/280 and 260/230 ratios as a measure of purity.

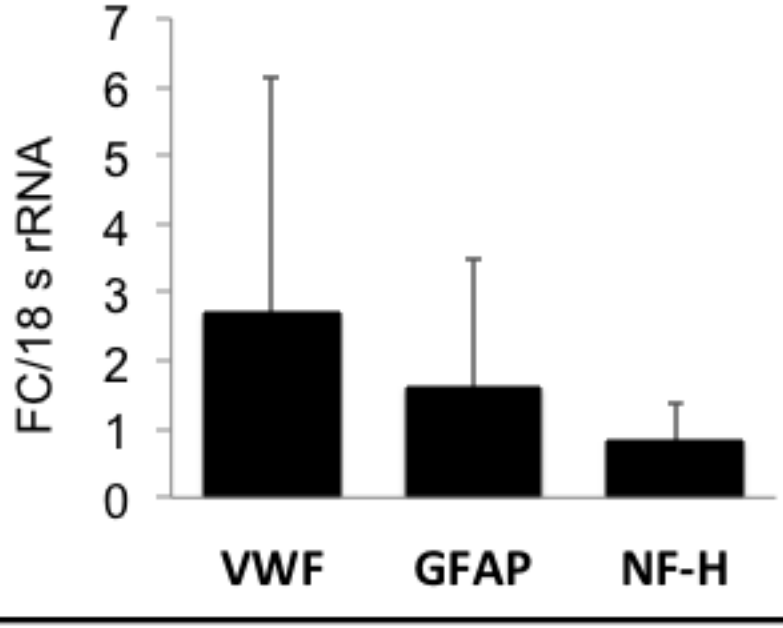

Figure 18. Expression of cell specific markers in laser captured collaterals. To verify specificity of captured elements, endothelial cell (VWF), and glial marker (GFAP), neuronal (NF-H) expression were checked by RT-PCR.

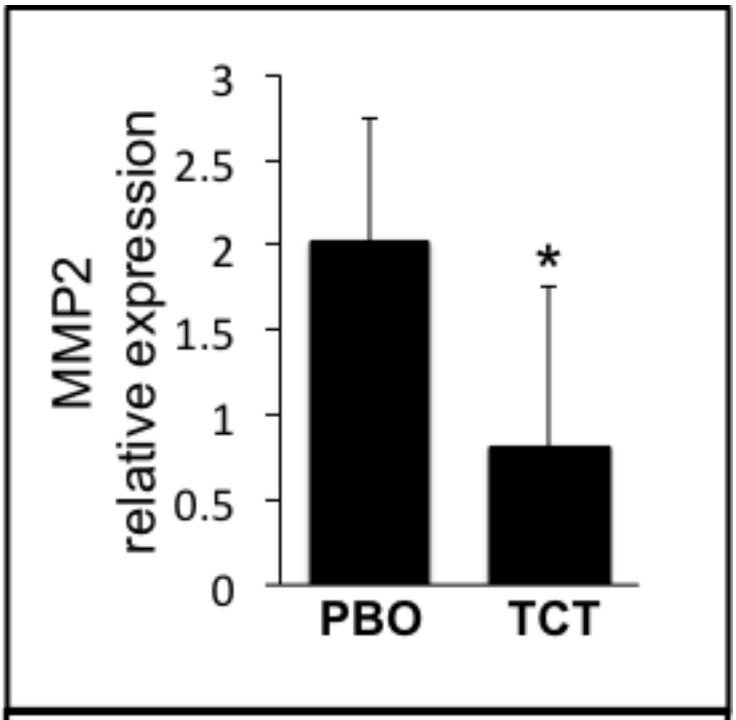

Figure 19. MMP2 mRNA expression from laser captured collaterals. Expression of MMP was validated using real-time PCR in captured vessels of TCT supplemented animals versus placebo control group. *$p<0.05$

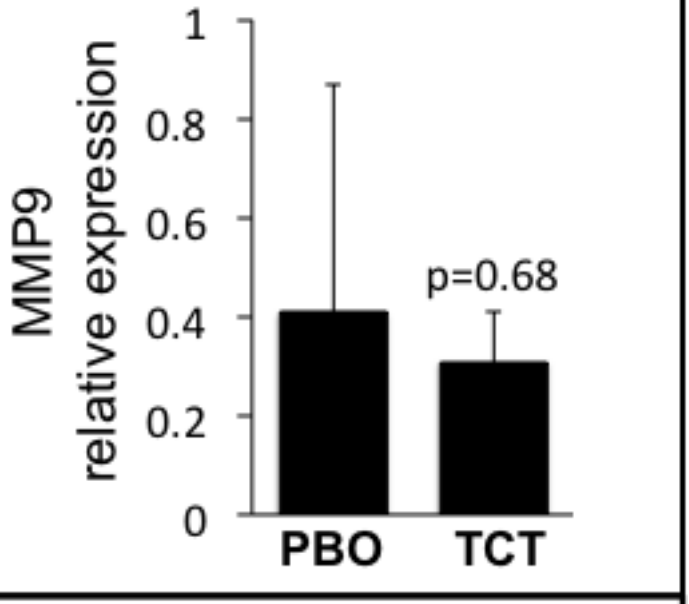

Figure 20. MMP9 mRNA expression from laser captured collaterals. Expression of MMP9 was validated using real-time PCR in captured vessels of TCT supplemented animals versus placebo control group.

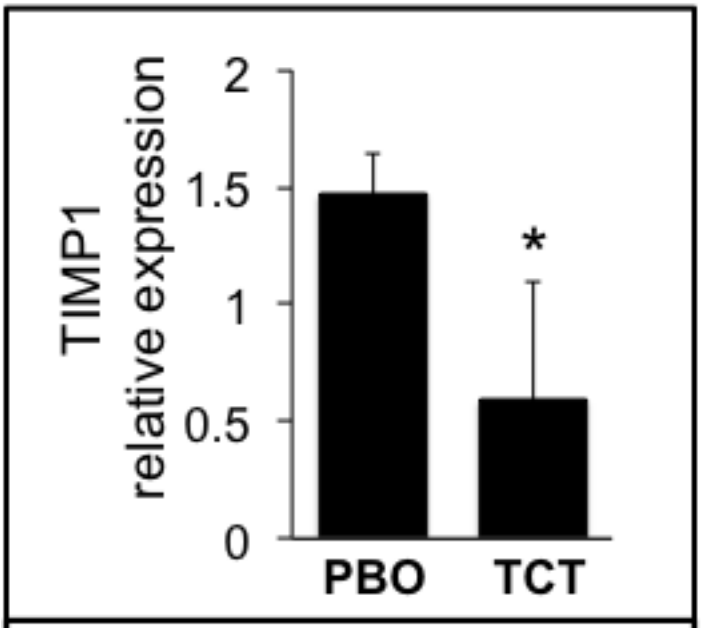

Figure 21. TIMP1 mRNA expression from laser captured collaterals. Expression of TIMP1 was validated using real-time PCR in captured vessels of TCT supplemented animals versus placebo control group. *$p<0.05$

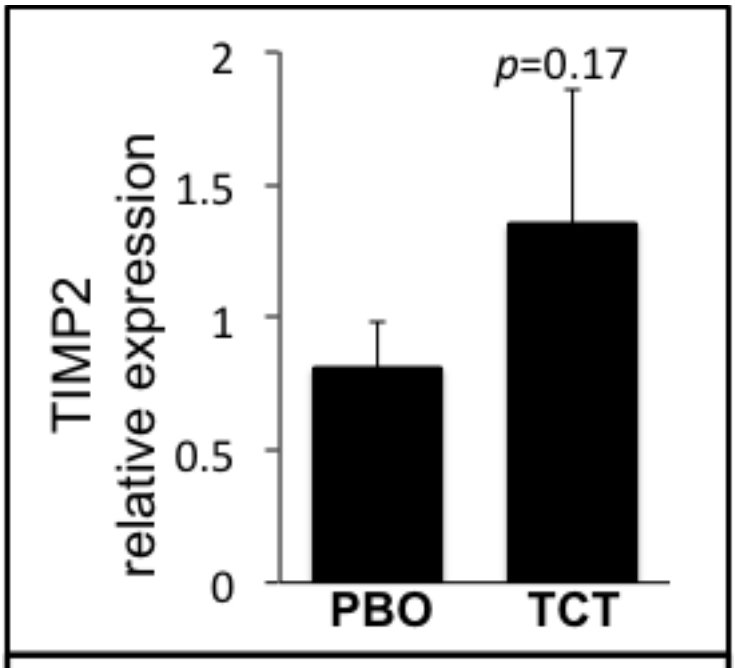

Figure 22. TIMP2 mRNA expression from laser captured collaterals. Expression of TIMP2 was validated using real-time PCR in captured vessels of TCT supplemented animals versus placebo control group.

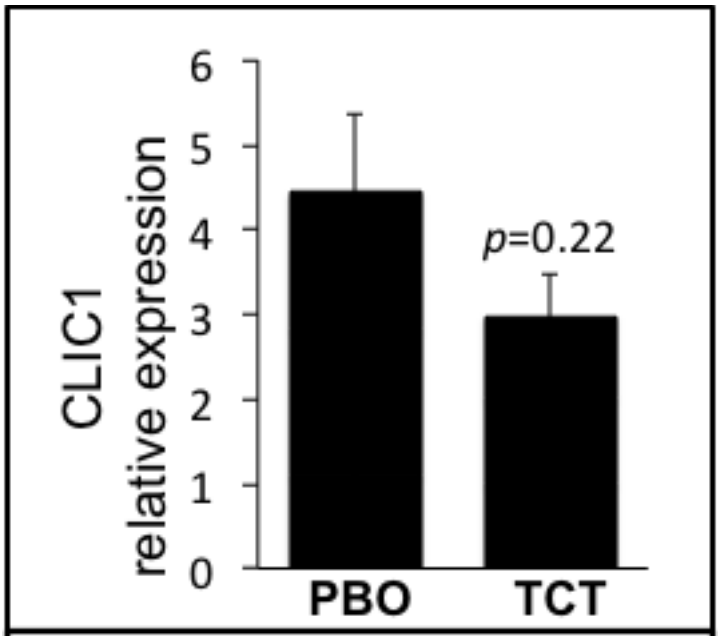

Figure 23. CLIC1 mRNA expression from laser captured collaterals. Expression of CLIC1 was validated using real-time PCR in captured vessels of TCT supplemented animals versus placebo control group.

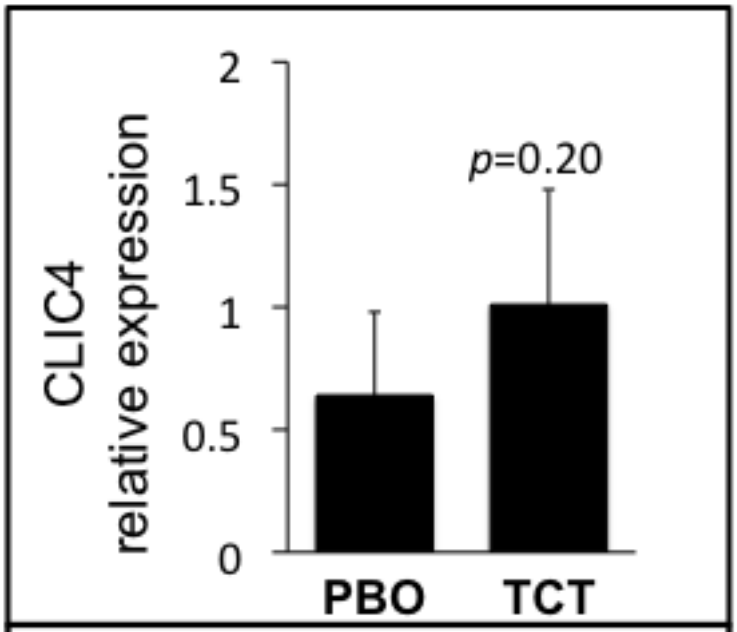

Figure 24. CLIC4 mRNA expression from laser captured collaterals. Expression CLIC4 was validated using real-time PCR in captured vessels of TCT supplemented animals versus placebo control group.

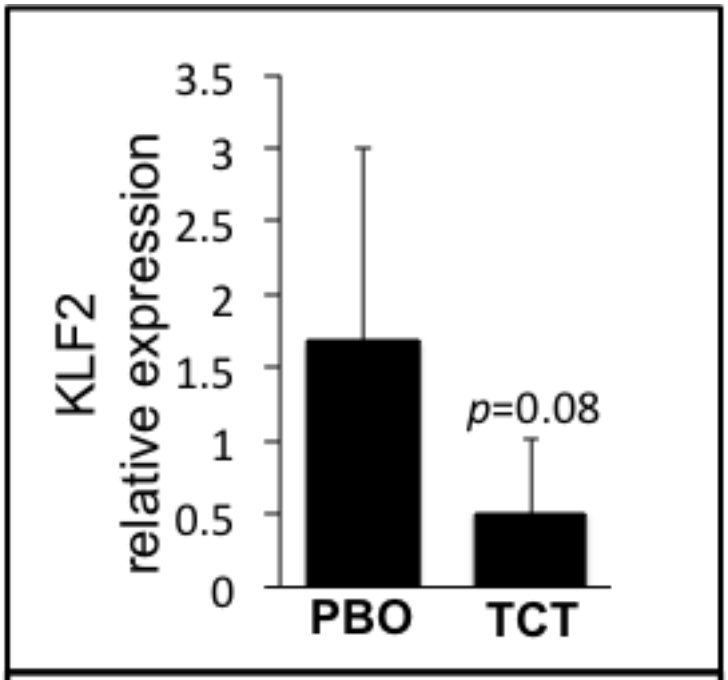

Figure 25. KLF2 mRNA expression from laser captured collaterals. Expression of KLF2 was validated using real-time PCR in captured vessels of TCT supplemented animals versus placebo control group.

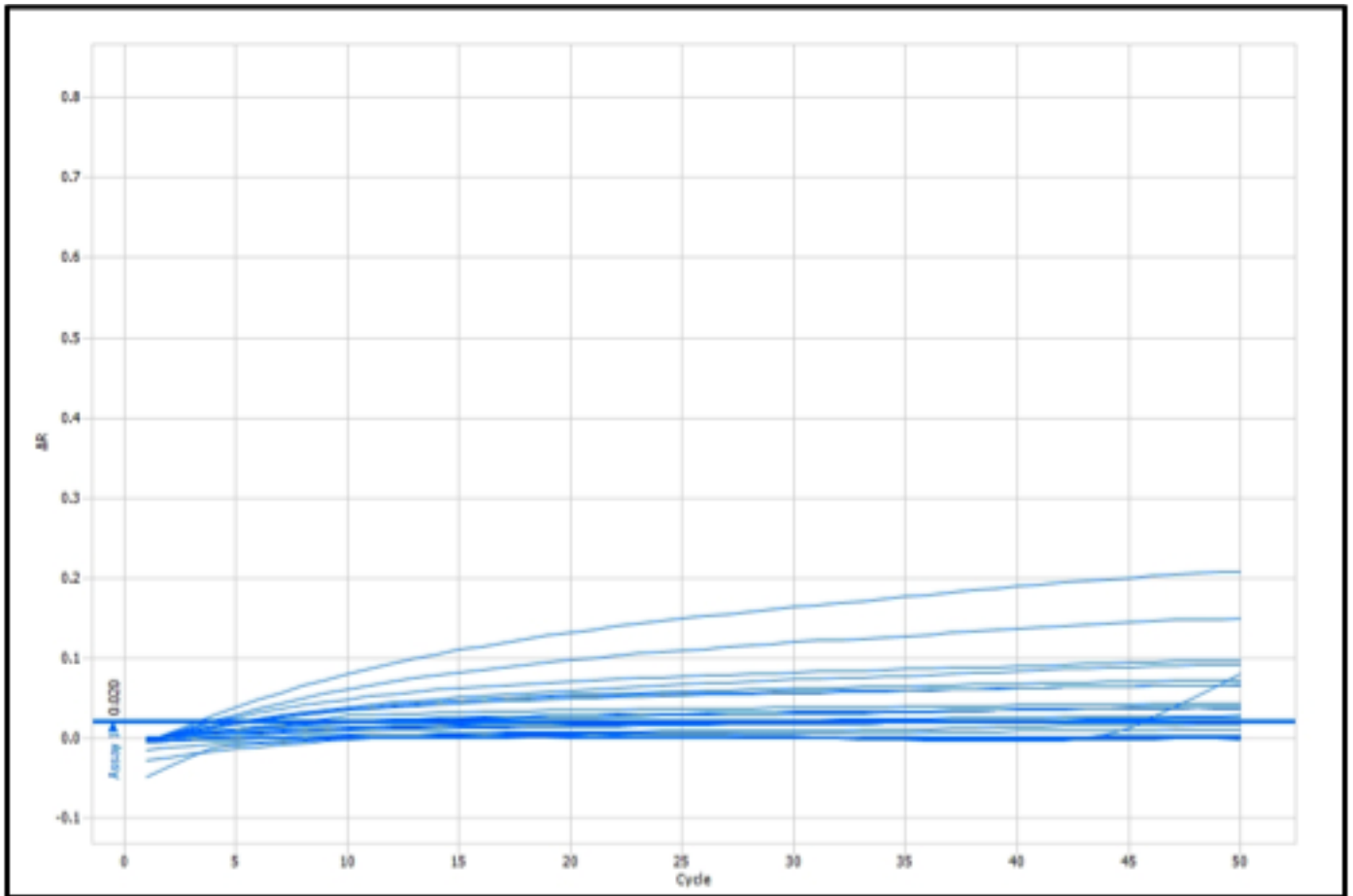

Figure 26. RT-PCR amplification plot of CD44v3. Review of CD44v3 amplification plot demonstrates no amplification with the exception of one sample, in which very late amplification was observed. This outcomes suggests either CD44v3 is not expressed in perfused collaterals of mouse, or ineffective primer design. The latter is likely not the case, as we used a published mouse primer[53].

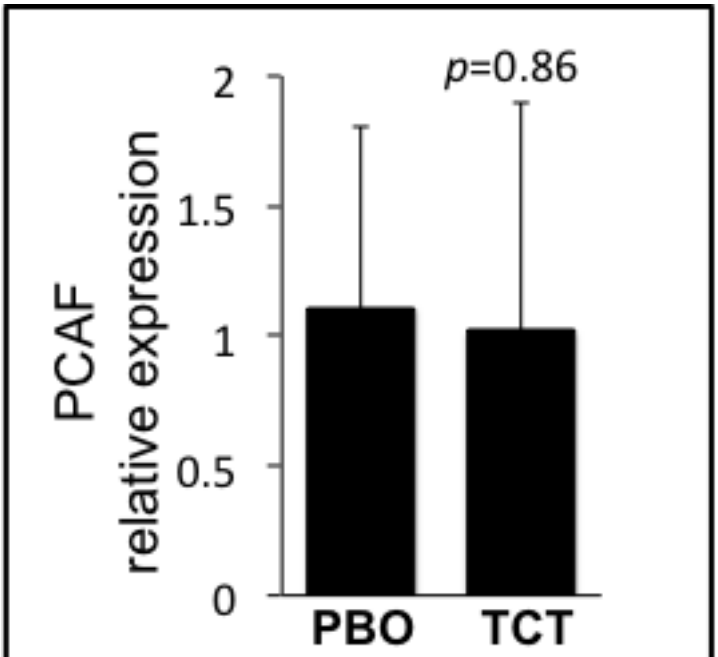

Figure 27. PCAF mRNA expression from laser captured collaterals. Expression of PCAF was validated using real-time PCR in captured vessels of TCT supplemented animals versus placebo control group.

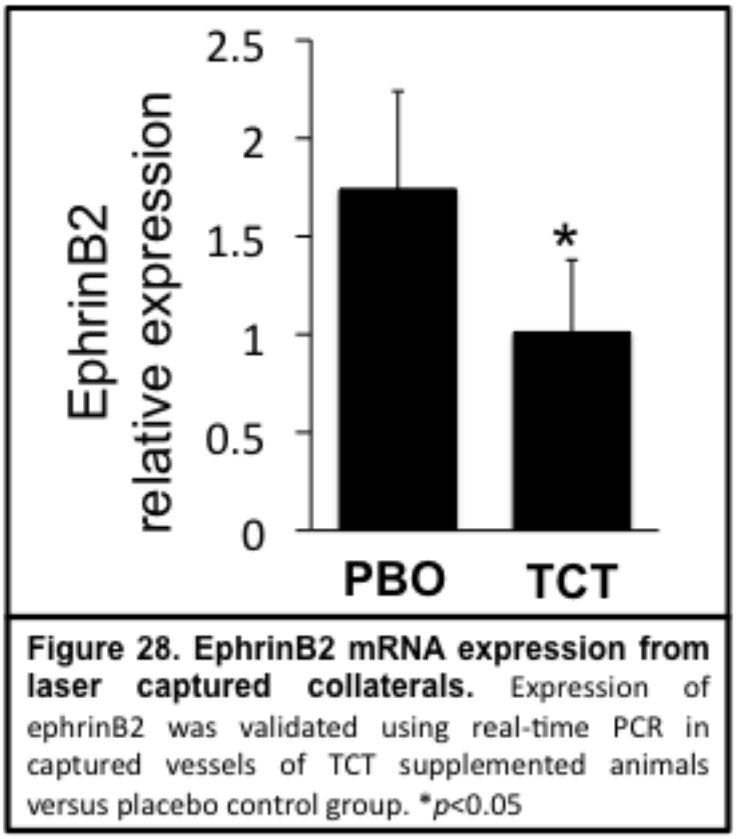

Figure 28. EphrinB2 mRNA expression from laser captured collaterals. Expression of ephrinB2 was validated using real-time PCR in captured vessels of TCT supplemented animals versus placebo control group. *$p<0.05$

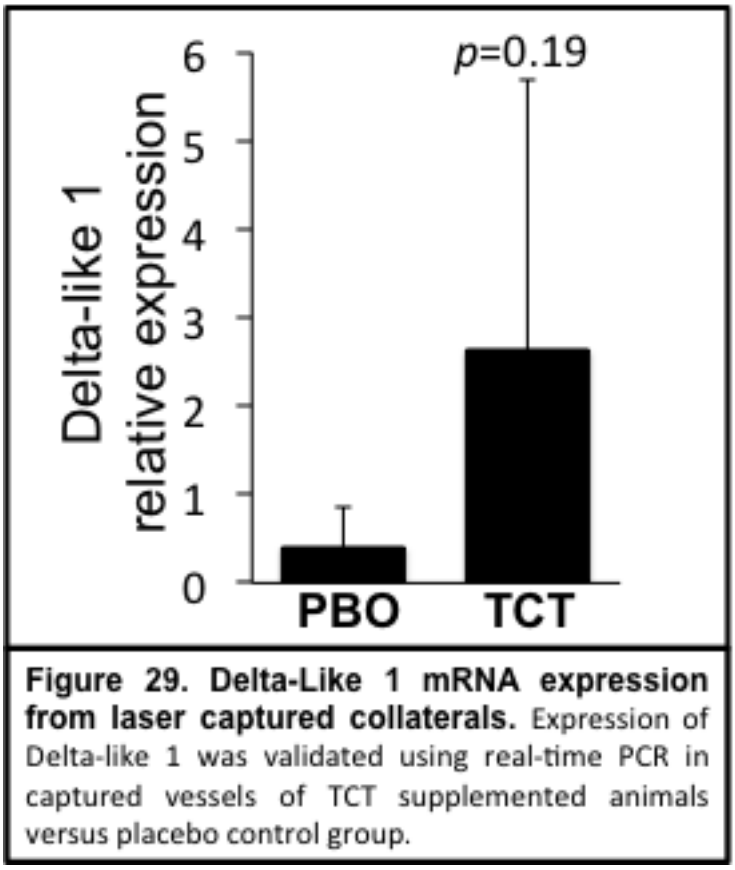

Figure 29. Delta-Like 1 mRNA expression from laser captured collaterals. Expression of Delta-like 1 was validated using real-time PCR in captured vessels of TCT supplemented animals versus placebo control group.

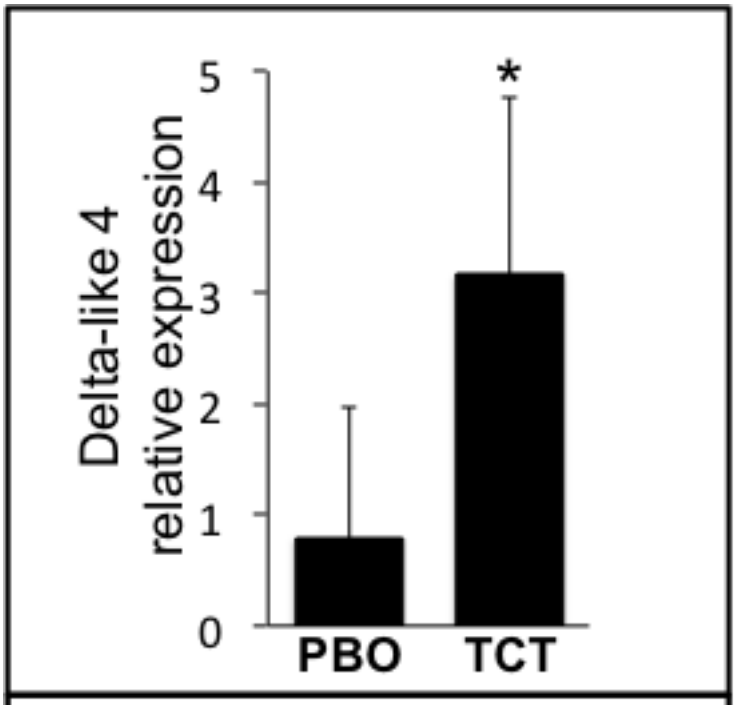

Figure 30. Delta-Like 4 mRNA expression from laser captured collaterals. Expression of Delta-like 4 was validated using real-time PCR in captured vessels of TCT supplemented animals versus placebo control group. *$p<0.05$

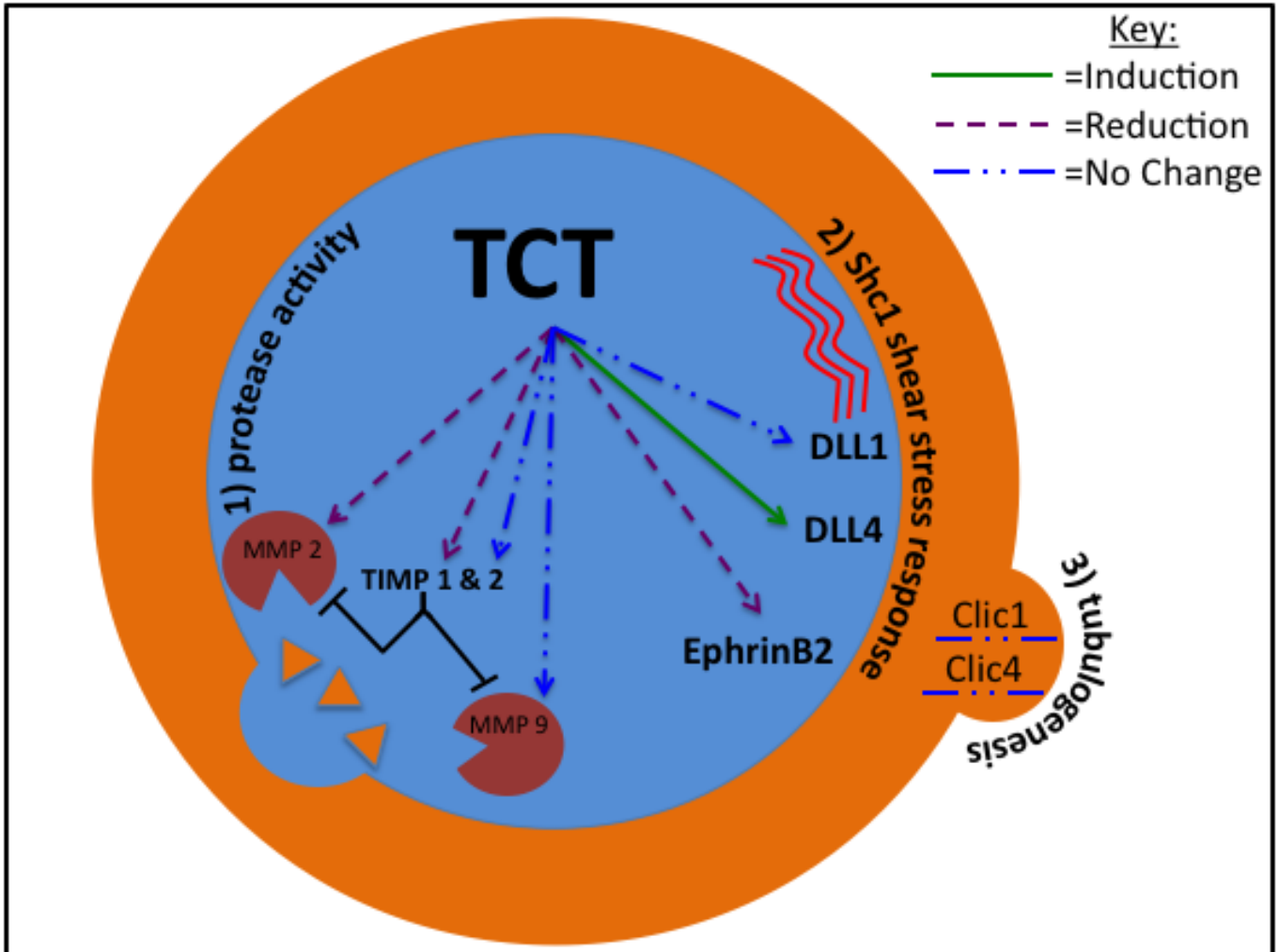

Figure 31. Schematic representation of arteriogenesis and the studied markers. This schematic shows the different role of each of the genetic markers screened in this study. Their implicated role in the arteriogenic process is show. TIMPs and MMPs are associated with protease activity. Shc1 related shear stress response pathways include DLL1, DLL4, and Ephrin2B genes. CLIC genes are heavily expressed in endothelial cells, and implicated in the process of tubulogenesis, imperative for vascular remodeling. Both show no change in response 4 week to TCT supplementation.

Discussion:

The motivation for ischemic stroke research is driven by the paucity of clinically available therapies for stroke patients. While a number of stroke therapies have shown promise in pre-clinical testing, few have proven effective in a clinical setting[60]. A recent review of 8,516 stroke related studies identified 1,026 candidates in pre-clinical testing that showed promise for treatment of ischemic stroke[61]. To date, each of these have fallen short in clinical trials[62]. Due to this grave need for therapeutic options to treat ischemic stroke patients, we set about testing TCT against ischemic stroke. Our lab has been studying tocotrienol vitamin E isoforms in the context of neuroprotection against ischemic stroke for over a decade[11,21,29,31,37,63-73]. As a natural vitamin, humans have safely consumed tocotrienols as part of a complex diet for centuries[74,75]. The most abundant natural source of TCT vitamin E comes from palm oil. Palm oil is predominantly produced in Malaysia and Indonesia, which account for around 85% of the world's palm oil[76]. As the world's principal producer of palm oil, the palm oil plant is significant to the agriculture and economy of both Maylasia and Indonesia. In Malaysia the palm oil industry accounts for 3.2% of the national GDP and 6 to 7% of the national GDP in Indonesia[77]. Recently, palm oil derived tocotrienol vitamin E has been granted Generally Recognized As Safe (GRN No. 307) certification by the United States Food and Drug Administration (U.S. FDA) for use as a food ingredient[78]. In light of a robust safety profile and growing body of research testing mechanisms of both neuro- and vascular-protection, we have begun clinical testing of tocotrienol vitamin E in patients who already suffered a sentinel ischemic stroke (*see* NCT01578629 on

clinicaltrials.gov). This patient population is at high risk for a second stroke event within one year of their first stroke episode, therefore serving as an ideal population of study for a prophylactic intervention such as TCT. This work, returns to pre-clinical testing to elucidate mechanisms of the vascular protective properties of TCT against acute ischemic stroke. Outcomes may direct future clinical trial designs that specifically target vascular protective intervention, such as catheter based delivery or long-term prophylactic dietary supplementation.

In light of the failure for putative stroke therapeutics that found success in rodent pre-clinical testing but failed in human clinical trials, we sought to test TCT against ischemic stroke in a large animal model that more closely approximated the human stroke condition. The mongrel canine stroke model required two small femoral artery punctures, followed by insertion of a platinum embolic coil to occlude the middle cerebral artery, as confirmed by c-arm fluoroscopy[79]. This testing showed that TCT does attenuate stroke-induced injury in a canine brain that more closely approximates that of a human. This study also uncovered an important clue into a previously unknown mechanism for TCT protection against stroke-induced brain injury. Specifically, cerebral angiograms enabled in our large animal setting demonstrated that TCT but not placebo treated canines possessed increased collateral blood flow in the stroke hemisphere. This observation was the first to identify a TCT-dependent vascular protection mechanism against stroke-induced injury[31]. As no new vessels were seen within the angiogram, the protection was understood to take place via remodeling of pre-existing collaterals, a process referred to as arteriogenesis. On the basis of this observation, we

move back to the mouse in order to more easily study the mechanisms of collateral remodeling identified in our large animal, canine stroke model. The mouse is better suited for this study because of decreased cost associated with the model, increased availability of test subjects, and access to molecular biology reagents for testing purposes.

Our first step when moving to a mouse model was to validate the improvement in collaterals observed in canine testing. To do so, an identical supplementation experimental design was employed for mice. They were supplemented for 10 weeks, then given stroke and compared to their placebo counterpart for both infarct volumes as well as blood flow to the stroke-affected hemisphere. Real time angiography was not feasible in mouse, as their smaller size limits fluoroscopy exposure. Therefore, in order to verify an increase in blood flow, laser speckle contrast imaging was employed. Laser speckle contrast imaging work by shining a laser on the surface of the cortex, causing the light to scatter and produce a speckle pattern that can be captured by a camera. Analysis of the speckle pattern leads to a so called “speckle contrast”, which is then related to a measure of blood flow for each area of the cortex[80,81]. Results showed that 10 week prophylactic TCT significantly increased blood flow in the stroke-affected tissue as compared to PBO supplemented controls. Furthermore, stroke-induced lesion volume was attenuated as measured by 11.7T MRI. These outcomes were consistent with results observed in our published canine work[31] (**Figures 30, 31**).

From here we began to study the mechanistic basis for this arteriogenic cerebrovascular remodeling we had seen in both the canine and mouse model. One of the first questions that arose was the time frame of supplementation required for this process to be effective. As we observed successful remodeling and improved collateral circulation during stroke in mice supplemented with TCT at 10 weeks, we elected to also study an earlier time frame of 4-6 weeks to detect earlier changes in gene expression that may affect the long acting improvement in blood flow during stroke. Originally, we had proposed to separate the two groups into separate time points and compare the two, however there was no significant different in vascular changes seen between the groups, so they were joined together as one earlier time point trial. By doing this, we aimed to shed light on the temporal resolution of the arteriogenic transcriptome, by comparing pro-arteriogenic markers studied at the 10 week time point of the published canine study to the 4-6 week time point. In addition to the few genetic markers studied in the 10 week study, we also identified new pro-arteriogenic candidates for their sensitivity to TCT supplementation after 4 weeks.

Importantly, this is the first work to test vitamin E levels in brain as early as 4 weeks after start of supplementation. Results revealed that the concentration of alpha-tocotrienol in brain after one month of supplementation is sufficient to afford neuroprotection on the basis of previously published work[39,67]. We hypothesize that this amount is also adequate to induce vascular remodeling. As it relates to vascular protection here, TCT supplementation significantly decreased TIMP1 expression in perfused vessels of the stroke-affected primary somatosensory cortex. TIMP1's ability

to control extracellular matrix degradation and advancing vascular remodeling by the activation of cell proliferation represents an important role in arteriogenesis[33]. The observation that this supplementation may decrease TIMP1 expression in the blood vessel of stroke-affected hemisphere points to the possibility that oral supplementation of TCT may prime the cerebral vasculature, enabling arteriogenesis in response to an ischemic event in the cerebral cortex. Our understanding is that the onset of the arteriogenic remodeling process is marked by an initial decrease in expression of the protease inhibitor TIMP1. The targets of TIMP1, MMP2 and MMP9, belong to a class of MMPs known as gelatinases, which are unique from the other MMPs in their role as proteolytic enzymes. This class is capable of breaking down gelatin and type IV collagen found in the basal lamina, a layer of extracellular matrix secreted by the endothelial cells[82,83]. This process requires break down of the basal lamina to increase vessel diameter. Proteolysis of the internal and external basal lamina by MMPs is essential to overcome the structural barriers to growth[84-87]. The controlled breakdown of this vascular framework allows for the expansion and outward growth of collateral vessels[32], necessary for remodeling. Though previous work has suggested that at 10 weeks TIMP1 is significantly increased[31,33], our outcomes point to an acute phase decrease in TIMP1 that allows for more MMP2 and MMP9 gelatinase activity. This early response likely aids the remodeling process, while a late-phase (*i.e.* 10 weeks) increase in TIMP1 would help stabilize the functional vessel and prevent further remodeling or other break down leading to leakiness within the vessel. Overall, this work provides further evidence of TCT supplementation regulating TIMP1 expression and subsequently invoking cerebrovascular arteriogenesis.

In addition to TCT supplementation exerting influence over the proteolytic environment during cerebrovascular remodeling, it also appears to affect shear stress and related mechanotransduction signaling involved in the process of arteriogenesis. Previous work identified Shc1 as a shear-stress sensitive inducer of arteriogenesis[59]. Phosphorylated Shc1 adaptor protein is responsible for activating multiple tyrosine kinases, including Ras and MAPK which are believed to induce transcriptional activation of Notch ligands (*i.e.* Delta-like ligands 1 and 4)[59,88,89]. Shc1 is required for shear stress induced activation of these targets[59], so to indirectly study this adaptor protein we assessed mRNA expression of mechanotrasnduction-sensitive notch ligands, including DLL1 and DLL4. Interestingly, our results show DLL4 mRNA is significantly up-regulated (3.96x increase) by TCT supplementation, while DLL1 shows a trend of increased expression (6.44x increase, p=0.194). It would be expected that an increase in DLL1 and DLL4 mRNA expression would drive a concomitant increase in ephrinB2 expression. Here, no such effect was observed, suggesting the following possible explanations: (1) the time point for collection preceded DLL1 and DLL4 dependent induction of ephrinB2 in the notch signaling pathway, (2) post-transcriptional silencing of ephrinB2 by unknown mechanisms, (3) post-translational degradation of DLL1 and DLL4 protein, or (4) interference of DLL1/DLL4 notch ligand binding. Recent research on DLL1 and DLL4 show they have separate function. Pertinent literature shows that DLL1 is essential for proper function of shear stress induced arteriogenesis in the post-natal mouse[90], while DLL4 is only expressed in microvessels of the post-natal mouse, or all vessels during embryonic development[91]. In this light, TCT-dependent induction of DLL4 suggests two

possibilities: (1) that the majority of laser captured elements were smaller microvessels (capillaries, Ø<10μm → arterioles, Ø=10-50μm), or (2) that TCT supplementation is leading to a "reprogramming" of endothelial cells, awakening normally dormant embryonic development genes such as DLL4. Overall, we hypothesize that an increase in Shc1 expression has occurred, due to the up-regulation of its closest studied downstream targets, DLL1 and DLL4. On the basis of these results, there is a clear need to study molecular target upstream of the delta-like ligands, specifically Shc1. To gain a better understanding of the role TCT supplementations is playing here, analysis of Shc1 mRNA and protein is required. To do so, Shc1 mRNA expression can be tested using real-time quantitative-PCR, protein expression can be tested using either Western Blot techniques or immunohistochemical staining, and finally protein activity can be determined by stoichiometric quantification of phosphorylated enzyme (active) compared to un-phosphylated enzyme (inactive)[92]. Due to the findings here, future experiments will address the notch signaling pathway in greater detail to further uncover the role it plays in shear stress induced arteriogenesis.

In addition to DLL1, DLL4, and ephrinB2, we investigated another pro-arteriogenic target known to be induced by shear stress and mechanotransduction signaling. KLF2 acts as an important transcriptional regulator of many processes within the body including cell proliferation, apoptosis, differentiation and development[93,94]. Relevant to this study, KLF2 is known as a shear stress-induced transcription factor capable of activation many proteins[95]. Critically, these proteins have anti-inflammatory as well as anti-coagulant properties. KLF2 is able to respond to shear stress by binding of

transcription factors to its promoter region. Many of the transcriptional factors are components of the shear stress regulatory complex, such as the coactivator PCAF[96]. Binding of these factors leads to the increased expression of KLF2 due to the increase in shear stress associated with ischemia[97,98]. Confirming this, work has been done to show that indeed a significant up-regulation of KLF2 is seen when high stress environments are applied for long periods of time[99]. The downward trend in expression of the KLF2 mRNA seen here indicated a decrease in shear stress has occurred. This suggests that 4 weeks of supplementation is sufficient to cause arteriogenic remodeling, resulting in an increase in vessel diameter and therefore a decrease in shear stress. Interestingly, findings have highlighted KLF2's ability to regulate hypoxia inducible factor 1-alpha (HIF-1α), as KLF2 promotes the degradation of HIF-1α[100]. Research on HIF-1α has shown that at an early time point, such as 30 minutes, increased HIF-1α expression is neuroprotective[101]. This additional mode of neuroprotection gives possible explanation to the decrease in KLF2 mRNA seen here. To test shear stress directly we plan to continue ongoing research using ultrasound to measure blood flow and corrosion cast to find diameter of the vessels, allowing for quantification of shear stress. The trend was very close to significance, and we believe that additional future additional test subject would be enough to make this statistic significant. Lastly targeted for its role in arteriogenesis through shear stress is PCAF. This transcriptional coactivator acts as a master switch equipped with histone acetyltransferase activity[57]. PCAF can acetylate both histone proteins and modulate nonhistone proteins, including those of the notch pathway mentioned previously[102]. Results here show a lack of response to TCT supplementation.

Another group of markers tested in this study were the chloride intracellular channel (CLIC) genes. Our previous research in a canine model has also indicated that CLICs are sensitive to TCT supplementation. There is also research to show CLICs role in collateral reformation[31,103]. These Chloride intracellular channel proteins are required for endothelial cell hollowing[50], which is essential for the vascular remodeling process. With this, we tested both CLIC1 and CLIC4 in the 4-week supplementation study. Our current work revealed no change in mRNA expression for either of the CLIC markers.

The current work leverages laboratory expertise with complex surgical models (rodent MCAO) and cutting edge technologies for cell and site specific resolution of tissue biology (Laser Capture Microdissection). While these approaches strengthen the work overall, they are not without their own limitations which are considered here. First and foremost, our surgical stroke model possesses strengths and weaknesses, which have been widely studied[104-107]. An advantage of the intraluminal suture model of middle cerebral artery occlusion is that it demonstrates a very good representation of ischemic stroke in nature. The method allows the restoration of blood flow after the induction of ischemia, which mimics the series of events in human stroke and allows for assessment of reperfusion[108], though this is not utilized in our project, as we euthanized during ischemia. Additionally, this is the most widely used stroke model in research, allowing for widespread comparison to other stroke research[109]. Limitations of the model include variability of infarct size and location, high mortality rate, hemmorraging[107], and all

complications that may result from a surgical procedure such as infection, immunodepression[110,111], hyperthermia[112,113], and loss of body weight[114,115]. Despite all of these limitations, the MCAO stroke model is still the most widely used and reproducible rodent model for acute ischemic stroke research. Of note, our laboratory takes additional measures to improve reproducibility and mitigate some of the aforementioned limitations. The use of laser doppler flowmetry is utilized to measure decrease in blood flow. This allows for increased consistency in the size and location of stroke.

Our use of laser capture microdissection also warrants consideration. One benefit of this technique in relation to our study, is that it allows for selective isolation of endothelial tissue. Without this, we would be forced to use whole tissue, and have to deal with much larger contamination of samples by non-specific glial and neuronal cells. Overall, this selective extraction of desired cells from heterogeneous tissues allows for improved subsequent molecular analyses[116]. As this technique allows for increased selectivity in cell type, it results in increased specificity of isolated RNA for downstream testing[117]. This technique also comes with inherent downside. One such negative is degradation of RNA due to slide handling and procurement procedures. As necessitated by our protocol, slides and tissue are exposed to solutions required for dehydration, staining, and other preparations as outlined in materials and methods. All of these steps pose increased risk and time of exposure to RNase activity. To combat these risks, we treat slides with RNase*Zap* (Ambion, Austin, TX, USA) before sectioning, and used RNA*later* (Ambion, Austin, TX, USA) once sections are mounted on the slides. Both

these techniques aid in the inactivation of RNase activity, aiding in the stabilization of the RNA. The entire LCM process requires a large amount of time while on the microscope, subjecting samples to greater risk of RNA degradation. In recognition of this limitation, for the current study we limited collection of endothelial cells to 30min per slide. Another problem is the amount of tissue collected. As the technique calls for selection of only specific cell types, the amount of tissue collected for downstream testing is vastly decreased as compared to ground whole tissue preparations. The decrease in tissue quantity is mirrored by lower RNA yields, leading to difficulties with further analysis of gene expression. To minimize these issues we optimized our protocol for collection for up to 2.1*10^5 μm^2. We also sought to increase the amount of tissue collected by increasing section thickness to 12 μm. These strategies allowed for successful yields of RNA necessary for downstream testing.

Our novel immunohistological approach using CD31 and FITC-lectin staining of analyzing for quantification of stroke must also be considered. The approach enables visualization of perfused vessels in the stroke-affected hemisphere along with direct comparison to the contralateral hemisphere. Through immunohistochemical analyses, this approach provides quantitative analyses of collateral improvement in the stroke-affected hemisphere. On the other hand, these staining techniques are not always accurate, and it is possible that not every vessel was stained. Contributing to this, there is a varied amount of endothelial cell markers present in the vascular bed, and this is constantly in fluctuation due to a combination of factors, including vessel size, anatomical compartment differences within organ, and presence of pathological

conditions[118]. In addition to the staining of vessels, the software program that analyzes the stains has limitations. The program uses automated selection and quantification processes that can over- or under-estimate vessels that can be seen by the user, or mark background stain that are not indicative of a stained vessel as intended. To combat this the mosaic images used on the scope have been adjusted to maximize the software's recognition of stained regions.

Now with our insight into the outcomes from mRNA gene expression analyses, we have new testable hypotheses and strong starting points for additional studies to be conducted in the future. First we plan to look at activity of pro-arteriogenic enzymes identified here and listed throughout this discussion. An understanding of enzyme activity will help shed greater light on the how it is that TCT is able to induce arteriogenic remodeling of cerebrovasculature. These future studies hold grave importance in both the protease and shear stress pathways studied within this research. Secondly, use of corrosion casts to directly measure vessel growth and diameter hold great promise. With this information, as well as blood flow through larger vessels as measured by ultrasound, we could calculate shear stress, and directly measure its change throughout a study to see its overall effect. Finally, we will continue to study the role played by TIMP1 in both TCT supplementation and arteriogenesis. We plan to utilize TIMP1 knockout mice in order to test the significance of TIMP1 on stroke related damage. Of further interest is whether TCT supplementation in TIMP1 knockout still attenuates stroke-induced brain injury. If not, outcomes will suggest that TIMP1 is essential for TCT-mediated protection against stroke. Overall, the project provides new

insight into mechanisms of arteriogenesis in response to TCT supplementation, and gives direction to a multitude of future research projects.

References:

1. Go, A.S.*, et al.* Heart Disease and Stroke Statistics--2013 Update: A Report From the American Heart Association. *Circulation* **127**, e6-e245 (2013).

2. Milionis, H. & Michel, P. Acute ischemic cerebrovascular events on antiplatelet therapy: What is the optimal prevention strategy? *Curr Pharm Des* (2012).

3. Rhim, T., Lee, D.Y. & Lee, M. Drug Delivery Systems for the Treatment of Ischemic Stroke. *Pharm Res* (2013).

4. Zivin, J.A. Acute stroke therapy with tissue plasminogen activator (tPA) since it was approved by the U.S. Food and Drug Administration (FDA). *Ann Neurol* **66**, 6-10 (2009).

5. Kleindorfer, D.*, et al.* Eligibility for recombinant tissue plasminogen activator in acute ischemic stroke: a population-based study. *Stroke* **35**, e27-29 (2004).

6. Diener, H.C.*, et al.* Aspirin and clopidogrel compared with clopidogrel alone after recent ischaemic stroke or transient ischaemic attack in high-risk patients (MATCH): randomised, double-blind, placebo-controlled trial. *Lancet* **364**, 331-337 (2004).

7. Nishida, U.*, et al.* Evaluation of small bowel blood flow in healthy subjects receiving low-dose aspirin. *World J Gastroenterol* **17**, 226-230 (2011).

8. Rink, C.*, et al.* Tocotrienol vitamin E protects against preclinical canine ischemic stroke by inducing arteriogenesis. *J Cereb Blood Flow Metab* **31**, 2218-2230 (2011).

9. Kiple, K.F. & Ornelas, K.C. *The Cambridge world history of food*, (Cambridge University Press, Cambridge, UK ; New York, 2000).

10. Emerson, O.H., Emerson, G.A. & Evans, H.M. The Isolation from Cottonseed Oil of an Alcohol Resembling Alpha Tocopherol from Wheat Germ Oil. *Science* **83**, 421 (1936).

11. Sen, C.K., Khanna, S., Rink, C. & Roy, S. Tocotrienols: the emerging face of natural vitamin E. *Vitamins and hormones* **76**, 203-261 (2007).

12. Sundram, K., Sambanthamurthi, R. & Tan, Y.A. Palm fruit chemistry and nutrition. *Asia Pacific journal of clinical nutrition* **12**, 355-362 (2003).

13. Sarris, A. & Food and Agriculture Organization of the United Nations. *Medium-term prospects for agricultural commodities : projections to the year 2010*, (Food and Agriculture Organization of the United Nations, Rome, 2003).

14. McFerron, W. Record Global Palm Oil Output Seen Raising Vegetable Oil Supply. (ed. Carpenter, C.) (Bloomber, Bloomberg News, 2013).

15. Sundram, K., Hayes, K.C. & Siru, O.H. Dietary palmitic acid results in lower serum cholesterol than does a lauric-myristic acid combination in normolipemic humans. *The American journal of clinical nutrition* **59**, 841-846 (1994).

16. Ayorinde, F.O., Garvin, K. & Saeed, K. Determination of the fatty acid composition of saponified vegetable oils using matrix-assisted laser desorption/ionization time-of-flight mass spectrometry. *Rapid communications in mass spectrometry : RCM* **14**, 608-615 (2000).

17. Cater, N.B., Heller, H.J. & Denke, M.A. Comparison of the effects of medium-chain triacylglycerols, palm oil, and high oleic acid sunflower oil on plasma triacylglycerol fatty acids and lipid and lipoprotein concentrations in humans. *The American journal of clinical nutrition* **65**, 41-45 (1997).

18. Choudhury, N., Tan, L. & Truswell, A.S. Comparison of palmolein and olive oil: effects on plasma lipids and vitamin E in young adults. *The American journal of clinical nutrition* **61**, 1043-1051 (1995).

19. Ladeia, A.M., Costa-Matos, E., Barata-Passos, R. & Costa Guimaraes, A. A palm oil-rich diet may reduce serum lipids in healthy young individuals. *Nutrition* **24**, 11-15 (2008).

20. Pennock, J.F., Hemming, F.W. & Kerr, J.D. A reassessment of tocopherol in chemistry. *Biochemical and biophysical research communications* **17**, 542-548 (1964).

21. Sen, C.K., Rink, C. & Khanna, S. Palm oil-derived natural vitamin E alpha-tocotrienol in brain health and disease. *Journal of the American College of Nutrition* **29**, 314S-323S (2010).

22. Abbasi, A.R., Hajirezaei, M., Hofius, D., Sonnewald, U. & Voll, L.M. Specific roles of alpha- and gamma-tocopherol in abiotic stress responses of transgenic tobacco. *Plant physiology* **143**, 1720-1738 (2007).

23. Collakova, E. & DellaPenna, D. Homogentisate phytyltransferase activity is limiting for tocopherol biosynthesis in Arabidopsis. *Plant physiology* **131**, 632-642 (2003).

24. Hofius, D.*, et al.* RNAi-mediated tocopherol deficiency impairs photoassimilate export in transgenic potato plants. *Plant physiology* **135**, 1256-1268 (2004).

25. Horvath, G.*, et al.* Differential distribution of tocopherols and tocotrienols in photosynthetic and non-photosynthetic tissues. *Phytochemistry* **67**, 1185-1195 (2006).

26. Parker, R.A., Pearce, B.C., Clark, R.W., Gordon, D.A. & Wright, J.J. Tocotrienols regulate cholesterol production in mammalian cells by post-transcriptional suppression of 3-hydroxy-3-methylglutaryl-coenzyme A reductase. *The Journal of biological chemistry* **268**, 11230-11238 (1993).

27. Pearce, B.C., Parker, R.A., Deason, M.E., Qureshi, A.A. & Wright, J.J. Hypocholesterolemic activity of synthetic and natural tocotrienols. *Journal of medicinal chemistry* **35**, 3595-3606 (1992).

28. Nesaretnam, K., Guthrie, N., Chambers, A.F. & Carroll, K.K. Effect of tocotrienols on the growth of a human breast cancer cell line in culture. *Lipids* **30**, 1139-1143 (1995).

29. Khanna, S.*, et al.* Neuroprotective properties of the natural vitamin E alpha-tocotrienol. *Stroke; a journal of cerebral circulation* **36**, 2258-2264 (2005).

30. Packer, L., Weber, S.U. & Rimbach, G. Molecular aspects of alpha-tocotrienol antioxidant action and cell signalling. *The Journal of nutrition* **131**, 369S-373S (2001).

31. Rink, C.*, et al.* Tocotrienol vitamin E protects against preclinical canine ischemic stroke by inducing arteriogenesis. *Journal of cerebral blood flow and metabolism*

: official journal of the International Society of Cerebral Blood Flow and Metabolism **31**, 2218-2230 (2011).

32. Cai, W. & Schaper, W. Mechanisms of arteriogenesis. *Acta biochimica et biophysica Sinica* **40**, 681-692 (2008).

33. Hillmeister, P.*, et al.* Induction of cerebral arteriogenesis leads to early-phase expression of protease inhibitors in growing collaterals of the brain. *Journal of cerebral blood flow and metabolism : official journal of the International Society of Cerebral Blood Flow and Metabolism* **28**, 1811-1823 (2008).

34. Roy, S., Venojarvi, M., Khanna, S. & Sen, C.K. Simultaneous detection of tocopherols and tocotrienols in biological samples using HPLC-coulometric electrode array. *Methods in enzymology* **352**, 326-332 (2002).

35. Roy, S., Khanna, S., Nallu, K., Hunt, T.K. & Sen, C.K. Dermal wound healing is subject to redox control. *Molecular therapy : the journal of the American Society of Gene Therapy* **13**, 211-220 (2006).

36. Rink, C., Gnyawali, S., Peterson, L. & Khanna, S. Oxygen-inducible glutamate oxaloacetate transaminase as protective switch transforming neurotoxic glutamate to metabolic fuel during acute ischemic stroke. *Antioxidants & redox signaling* **14**, 1777-1785 (2011).

37. Rink, C.*, et al.* Oxygen-sensitive outcomes and gene expression in acute ischemic stroke. *Journal of cerebral blood flow and metabolism : official journal of the International Society of Cerebral Blood Flow and Metabolism* **30**, 1275-1287 (2010).

38. Hosomi, A.*, et al.* Affinity for alpha-tocopherol transfer protein as a determinant of the biological activities of vitamin E analogs. *FEBS letters* **409**, 105-108 (1997).

39. Khanna, S., Patel, V., Rink, C., Roy, S. & Sen, C.K. Delivery of orally supplemented alpha-tocotrienol to vital organs of rats and tocopherol-transport protein deficient mice. *Free radical biology & medicine* **39**, 1310-1319 (2005).

40. Panagabko, C.*, et al.* Ligand specificity in the CRAL-TRIO protein family. *Biochemistry* **42**, 6467-6474 (2003).

41. Newman, P.J.*, et al.* PECAM-1 (CD31) cloning and relation to adhesion molecules of the immunoglobulin gene superfamily. *Science* **247**, 1219-1222 (1990).

42. Newman, P.J. & Albelda, S.M. Cellular and molecular aspects of PECAM-1. *Nouvelle revue francaise d'hematologie* **34 Suppl**, S9-13 (1992).

43. Buschmann, I. & Schaper, W. The pathophysiology of the collateral circulation (arteriogenesis). *The Journal of pathology* **190**, 338-342 (2000).

44. Tronc, F.*, et al.* Role of matrix metalloproteinases in blood flow-induced arterial enlargement: interaction with NO. *Arteriosclerosis, thrombosis, and vascular biology* **20**, E120-126 (2000).

45. Viappiani, S.*, et al.* Activation and modulation of 72kDa matrix metalloproteinase-2 by peroxynitrite and glutathione. *Biochemical pharmacology* **77**, 826-834 (2009).

46. Ashley, R.H. Challenging accepted ion channel biology: p64 and the CLIC family of putative intracellular anion channel proteins (Review). *Molecular membrane biology* **20**, 1-11 (2003).

47. Tung, J.J., Hobert, O., Berryman, M. & Kitajewski, J. Chloride intracellular channel 4 is involved in endothelial proliferation and morphogenesis in vitro. *Angiogenesis* **12**, 209-220 (2009).

48. Waltenberger, J. Limits to growth of native collateral vessels: Just one mouse CLIC away from unlimited collateral perfusion? *Circulation research* **105**, 9-11 (2009).

49. Mehta, J.L. *Biochemical basis and therapeutic implications of angiogenesis*, (Springer, New York, 2013).

50. Ulmasov, B., Bruno, J., Gordon, N., Hartnett, M.E. & Edwards, J.C. Chloride intracellular channel protein-4 functions in angiogenesis by supporting acidification of vacuoles along the intracellular tubulogenic pathway. *The American journal of pathology* **174**, 1084-1096 (2009).

51. Boon, R.A.*, et al.* KLF2-induced actin shear fibers control both alignment to flow and JNK signaling in vascular endothelium. *Blood* **115**, 2533-2542 (2010).

52. Dekker, R.J.*, et al.* KLF2 provokes a gene expression pattern that establishes functional quiescent differentiation of the endothelium. *Blood* **107**, 4354-4363 (2006).

53. Basu, P.*, et al.* KLF2 is essential for primitive erythropoiesis and regulates the human and murine embryonic beta-like globin genes in vivo. *Blood* **106**, 2566-2571 (2005).

54. Lee, J.S.*, et al.* Klf2 is an essential regulator of vascular hemodynamic forces in vivo. *Developmental cell* **11**, 845-857 (2006).

55. Bot, P.T.*, et al.* Distinct CD44 splice variants differentially affect collateral artery growth. *Current vascular pharmacology* **11**, 13-20 (2013).

56. Goodfellow, P.N.*, et al.* The gene, MIC4, which controls expression of the antigen defined by monoclonal antibody F10.44.2, is on human chromosome 11. *European journal of immunology* **12**, 659-663 (1982).

57. Bastiaansen, A.J.*, et al.* Lysine acetyltransferase PCAF is a key regulator of arteriogenesis. *Arteriosclerosis, thrombosis, and vascular biology* **33**, 1902-1910 (2013).

58. Liu, Y., Sweet, D.T., Irani-Tehrani, M., Maeda, N. & Tzima, E. Shc coordinates signals from intercellular junctions and integrins to regulate flow-induced inflammation. *The Journal of cell biology* **182**, 185-196 (2008).

59. Sweet, D.T.*, et al.* Endothelial Shc regulates arteriogenesis through dual control of arterial specification and inflammation via the notch and nuclear factor-kappa-light-chain-enhancer of activated B-cell pathways. *Circulation research* **113**, 32-39 (2013).

60. Kidwell, C.S., Liebeskind, D.S., Starkman, S. & Saver, J.L. Trends in acute ischemic stroke trials through the 20th century. *Stroke; a journal of cerebral circulation* **32**, 1349-1359 (2001).

61. O'Collins, V.E.*, et al.* 1,026 experimental treatments in acute stroke. *Annals of neurology* **59**, 467-477 (2006).

62. Radermacher, K.A.*, et al.* The 1027th target candidate in stroke: Will NADPH oxidase hold up? *Experimental & translational stroke medicine* **4**, 11 (2012).

63. Khanna, S., Roy, S., Parinandi, N.L., Maurer, M. & Sen, C.K. Characterization of the potent neuroprotective properties of the natural vitamin E alpha-tocotrienol. *Journal of neurochemistry* **98**, 1474-1486 (2006).

64. Park, H.A.*, et al.* Glutathione disulfide induces neural cell death via a 12-lipoxygenase pathway. *Cell death and differentiation* **16**, 1167-1179 (2009).

65. Patel, V., Rink, C., Khanna, S. & Sen, C.K. Tocotrienols: the lesser known form of natural vitamin E. *Indian journal of experimental biology* **49**, 732-738 (2011).

66. Gohil, K., Roy, S., Packer, L. & Sen, C.K. Antioxidant regulation of gene expression: analysis of differentially expressed mRNAs. *Methods in enzymology* **300**, 402-410 (1999).

67. Khanna, S.*, et al.* Nanomolar vitamin E alpha-tocotrienol inhibits glutamate-induced activation of phospholipase A2 and causes neuroprotection. *Journal of neurochemistry* **112**, 1249-1260 (2010).

68. Khanna, S.*, et al.* Loss of miR-29b following acute ischemic stroke contributes to neural cell death and infarct size. *Journal of cerebral blood flow and metabolism :*

official journal of the International Society of Cerebral Blood Flow and Metabolism **33**, 1197-1206 (2013).

69. Khanna, S.*, et al.* Molecular basis of vitamin E action: tocotrienol modulates 12-lipoxygenase, a key mediator of glutamate-induced neurodegeneration. *The Journal of biological chemistry* **278**, 43508-43515 (2003).

70. Park, H.A.*, et al.* Natural vitamin E alpha-tocotrienol protects against ischemic stroke by induction of multidrug resistance-associated protein 1. *Stroke; a journal of cerebral circulation* **42**, 2308-2314 (2011).

71. Sen, C.K., Khanna, S. & Roy, S. Tocotrienol: the natural vitamin E to defend the nervous system? *Annals of the New York Academy of Sciences* **1031**, 127-142 (2004).

72. Sen, C.K., Khanna, S. & Roy, S. Tocotrienols in health and disease: the other half of the natural vitamin E family. *Molecular aspects of medicine* **28**, 692-728 (2007).

73. Sen, C.K., Khanna, S., Roy, S. & Packer, L. Molecular basis of vitamin E action. Tocotrienol potently inhibits glutamate-induced pp60(c-Src) kinase activation and death of HT4 neuronal cells. *The Journal of biological chemistry* **275**, 13049-13055 (2000).

74. Hartley, C.W.S. *The oil palm (Elaeis guineensis Jacq.)*, (Longman Scientific & Technical ;

Wiley, Harlow, Essex, England

New York, 1988).

75. Northrup, D. *Trade without rulers : pre-colonial economic development in south-eastern Nigeria*, (Clarendon Press, Oxford, 1978).

76. Sarif, E. Malaysia expected to maintain position as world's largest producer of Certified Sustainable Palm Oil in *The Star* (2011).

77. Levin, J. Profitability and Sustainability in Palm Oil Production. 60 (WWF, FMO and CDC, 2012).

78. Radzian, R. Palm oil-derived tocols with tocotrienols and α-tocopherol as the principal components (ed. FDA) (USA, 2010).

79. Rink, C.*, et al.* Minimally invasive neuroradiologic model of preclinical transient middle cerebral artery occlusion in canines. *Proceedings of the National Academy of Sciences of the United States of America* **105**, 14100-14105 (2008).

80. Briers, J.D. Laser Doppler, speckle and related techniques for blood perfusion mapping and imaging. *Physiological measurement* **22**, R35-66 (2001).

81. Yuan, S., Devor, A., Boas, D.A. & Dunn, A.K. Determination of optimal exposure time for imaging of blood flow changes with laser speckle contrast imaging. *Applied optics* **44**, 1823-1830 (2005).

82. McCawley, L.J. & Matrisian, L.M. Matrix metalloproteinases: they're not just for matrix anymore! *Current opinion in cell biology* **13**, 534-540 (2001).

83. Vu, T.H. & Werb, Z. Matrix metalloproteinases: effectors of development and normal physiology. *Genes & development* **14**, 2123-2133 (2000).

84. Hedin, U., Bottger, B.A., Forsberg, E., Johansson, S. & Thyberg, J. Diverse effects of fibronectin and laminin on phenotypic properties of cultured arterial smooth muscle cells. *The Journal of cell biology* **107**, 307-319 (1988).

85. Hedin, U., Bottger, B.A., Luthman, J., Johansson, S. & Thyberg, J. A substrate of the cell-attachment sequence of fibronectin (Arg-Gly-Asp-Ser) is sufficient to promote transition of arterial smooth muscle cells from a contractile to a synthetic phenotype. *Developmental biology* **133**, 489-501 (1989).

86. Palmberg, L., Claesson, H.E. & Thyberg, J. Effects of leukotrienes on phenotypic properties and growth of arterial smooth muscle cells in primary culture. *Journal of cell science* **93 (Pt 3)**, 403-408 (1989).

87. Thyberg, J. Differentiated properties and proliferation of arterial smooth muscle cells in culture. *International review of cytology* **169**, 183-265 (1996).

88. Ravichandran, K.S. Signaling via Shc family adapter proteins. *Oncogene* **20**, 6322-6330 (2001).

89. Sweet, D.T. & Tzima, E. Spatial signaling networks converge at the adaptor protein Shc. *Cell cycle* **8**, 231-235 (2009).

90. Limbourg, A.*, et al.* Notch ligand Delta-like 1 is essential for postnatal arteriogenesis. *Circulation research* **100**, 363-371 (2007).

91. Gale, N.W.*, et al.* Haploinsufficiency of delta-like 4 ligand results in embryonic lethality due to major defects in arterial and vascular development. *Proceedings of the National Academy of Sciences of the United States of America* **101**, 15949-15954 (2004).

92. Kosako, H. Phos-tag Western blotting for detecting stoichiometric protein phosphorylation in cells. *Nature Protocol Exchange* **170**(2009).

93. Pearson, R., Fleetwood, J., Eaton, S., Crossley, M. & Bao, S. Kruppel-like transcription factors: a functional family. *The international journal of biochemistry & cell biology* **40**, 1996-2001 (2008).

94. Weinreich, M.A.*, et al.* KLF2 transcription-factor deficiency in T cells results in unrestrained cytokine production and upregulation of bystander chemokine receptors. *Immunity* **31**, 122-130 (2009).

95. Huddleson, J.P., Ahmad, N. & Lingrel, J.B. Up-regulation of the KLF2 transcription factor by fluid shear stress requires nucleolin. *The Journal of biological chemistry* **281**, 15121-15128 (2006).

96. Ahmad, N. & Lingrel, J.B. Kruppel-like factor 2 transcriptional regulation involves heterogeneous nuclear ribonucleoproteins and acetyltransferases. *Biochemistry* **44**, 6276-6285 (2005).

97. Dekker, R.J.*, et al.* Prolonged fluid shear stress induces a distinct set of endothelial cell genes, most specifically lung Kruppel-like factor (KLF2). *Blood* **100**, 1689-1698 (2002).

98. Huddleson, J.P., Ahmad, N., Srinivasan, S. & Lingrel, J.B. Induction of KLF2 by fluid shear stress requires a novel promoter element activated by a phosphatidylinositol 3-kinase-dependent chromatin-remodeling pathway. *The Journal of biological chemistry* **280**, 23371-23379 (2005).

99. Janke, D.*, et al.* The "artificial artery" as in vitro perfusion model. *PloS one* **8**, e57227 (2013).

100. Kawanami, D.*, et al.* Kruppel-like factor 2 inhibits hypoxia-inducible factor 1alpha expression and function in the endothelium. *The Journal of biological chemistry* **284**, 20522-20530 (2009).

101. Shi, H. Hypoxia inducible factor 1 as a therapeutic target in ischemic stroke. *Current medicinal chemistry* **16**, 4593-4600 (2009).

102. Guarani, V.*, et al.* Acetylation-dependent regulation of endothelial Notch signalling by the SIRT1 deacetylase. *Nature* **473**, 234-238 (2011).

103. Chalothorn, D., Zhang, H., Smith, J.E., Edwards, J.C. & Faber, J.E. Chloride intracellular channel-4 is a determinant of native collateral formation in skeletal muscle and brain. *Circulation research* **105**, 89-98 (2009).

104. Yuan, F.*, et al.* Optimizing suture middle cerebral artery occlusion model in C57BL/6 mice circumvents posterior communicating artery dysplasia. *Journal of neurotrauma* **29**, 1499-1505 (2012).

105. Lipsanen, A. & Jolkkonen, J. Experimental approaches to study functional recovery following cerebral ischemia. *Cellular and molecular life sciences : CMLS* **68**, 3007-3017 (2011).

106. Belayev, L., Alonso, O.F., Busto, R., Zhao, W. & Ginsberg, M.D. Middle cerebral artery occlusion in the rat by intraluminal suture. Neurological and pathological evaluation of an improved model. *Stroke; a journal of cerebral circulation* **27**, 1616-1622; discussion 1623 (1996).

107. Braeuninger, S. & Kleinschnitz, C. Rodent models of focal cerebral ischemia: procedural pitfalls and translational problems. *Experimental & translational stroke medicine* **1**, 8 (2009).

108. Ringelstein, E.B.*, et al.* Type and extent of hemispheric brain infarctions and clinical outcome in early and delayed middle cerebral artery recanalization. *Neurology* **42**, 289-298 (1992).

109. Longa, E.Z., Weinstein, P.R., Carlson, S. & Cummins, R. Reversible middle cerebral artery occlusion without craniectomy in rats. *Stroke; a journal of cerebral circulation* **20**, 84-91 (1989).

110. Liesz, A.*, et al.* The spectrum of systemic immune alterations after murine focal ischemia: immunodepression versus immunomodulation. *Stroke; a journal of cerebral circulation* **40**, 2849-2858 (2009).

111. Meisel, C., Schwab, J.M., Prass, K., Meisel, A. & Dirnagl, U. Central nervous system injury-induced immune deficiency syndrome. *Nature reviews. Neuroscience* **6**, 775-786 (2005).

112. Morikawa, E.*, et al.* The significance of brain temperature in focal cerebral ischemia: histopathological consequences of middle cerebral artery occlusion in the rat. *Journal of cerebral blood flow and metabolism : official journal of the International Society of Cerebral Blood Flow and Metabolism* **12**, 380-389 (1992).

113. Zhao, Q., Memezawa, H., Smith, M.L. & Siesjo, B.K. Hyperthermia complicates middle cerebral artery occlusion induced by an intraluminal filament. *Brain research* **649**, 253-259 (1994).

114. Dittmar, M.S., Fehm, N.P., Vatankhah, B., Bogdahn, U. & Schlachetzki, F. Adverse effects of the intraluminal filament model of middle cerebral artery occlusion. *Stroke; a journal of cerebral circulation* **36**, 530-532; author reply 530-532 (2005).

115. Virtanen, T., Jolkkonen, J. & Sivenius, J. Re: External carotid artery territory ischemia impairs outcome in the endovascular filament model of middle cerebral artery occlusion in rats. *Stroke; a journal of cerebral circulation* **35**, e9-10; author reply e19-10 (2004).

116. Mojsilovic-Petrovic, J., Nesic, M., Pen, A., Zhang, W. & Stanimirovic, D. Development of rapid staining protocols for laser-capture microdissection of brain vessels from human and rat coupled to gene expression analyses. *Journal of neuroscience methods* **133**, 39-48 (2004).

117. Kerman, I.A., Buck, B.J., Evans, S.J., Akil, H. & Watson, S.J. Combining laser capture microdissection with quantitative real-time PCR: effects of tissue manipulation on RNA quality and gene expression. *Journal of neuroscience methods* **153**, 71-85 (2006).

118. Pusztaszeri, M.P., Seelentag, W. & Bosman, F.T. Immunohistochemical expression of endothelial markers CD31, CD34, von Willebrand factor, and Fli-1 in normal human tissues. *The journal of histochemistry and cytochemistry : official journal of the Histochemistry Society* **54**, 385-395 (2006).